The prediction of damage to masonry buildings caused by subsoil settlements

W. J. BERANEK
TNO-Institute for Building Materials and Structures

1 Introduction

The extraction of natural gas in the Province of Groningen in the northern Netherlands, is causing a dish-shaped subsoil settlement over an area of about 1000 km^2, see Fig. 1a and 1b. As a result the surface water level has to be adapted locally, see Fig. 1c and 1d. This in its turn produces a change in groundwater level, which can produce irregular settlements of the subsoil.

Such settlements will generally not endanger the stability of buildings, but might lower their serviceability, because of cracking in masonry walls. To reduce the probability of damage to a minimum, changes in the surface water level should be kept between certain limits; an investigation has been carried out to determine these limits [1].

The main parameters in this problem are:

- the constituency and properties of the subsoil;
- the geometry of the building and its foundations;
- the mechanical properties of the building materials;
- the magnitude and variation of the changes in groundwater level.

This paper presents a fundamental approach to determine the interaction between structure and subsoil due to the dead weight of the structure and changes in groundwater level. The approach is suitable for all kinds of structures, foundations and subsoil and can be used for all kinds of settlement and stress distribution formulas. In this paper the procedure has been worked out in detail for the case of a terrace of houses with footing foundations. This type of building, which is rather vulnerable to damage, is frequently found in this part of the country.

2 Groundwater

In large parts of the area being considered, the surface water level has been lowered more than one metre during the last 100 years. This has been done on the one hand to compensate for the natural settlements of the subsoil and on the other hand to improve agricultural conditions. In the future, variations in the surface water level are expected to be relatively small. In the investigation a lowering of the surface water level of 0.20 m has been used as a starting point.

A lowering of the surface water level will produce a fall in groundwater level. The groundwater level varies with the season and also is related to the constituency of the subsoil, the geometry of the parcel, the amount of rainfall, the evaporation and the amount of water withdrawn by vegetation. The daily groundwater level can be calculated using a computer program which takes into account the above factors. The

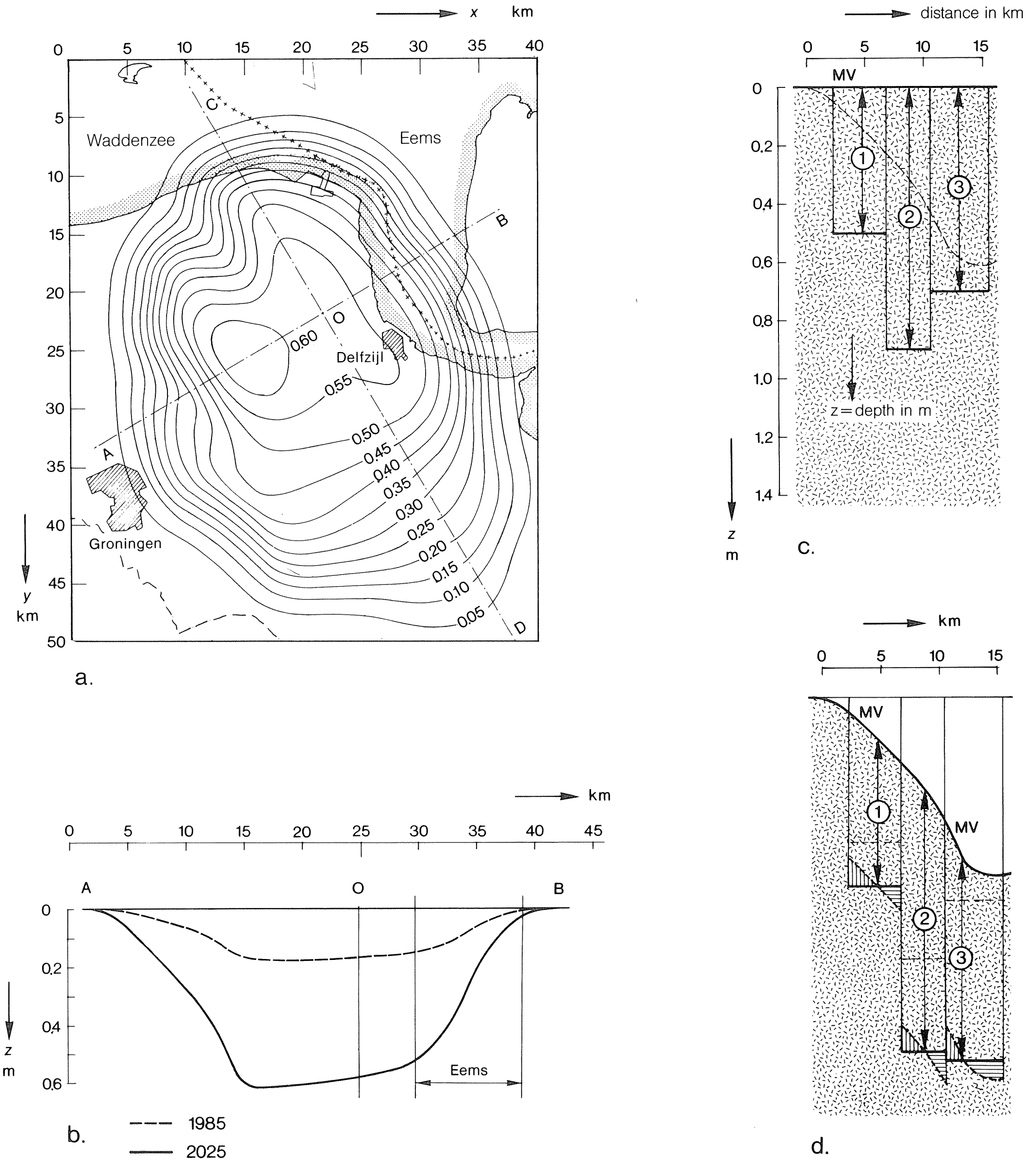

Fig. 1. Subsoil settlement in the Province of Groningen, caused by the extraction of natural gas.
a. Prognosis of settlements in the year 2025, shown as contour lines (settlement in m).
b. Settlements in Section A-B, see Fig. 1a, based on the prognoses for the years 1985 and 2025.
c. Surface water level in three adjacent polders before any settlements occurred.
d. Unchanged average of the surface water level relative to the ground level after settlements occurred.

MV = groundlevel.
① ② ③ = surface water level below groundlevel.

extreme situations for a long parcel in a wet winter and a very dry summer are shown in Fig. 2. In these calculations it has been assumed that the surface water level is the same in summer and in winter.

The effect of the surface water level lowered over 0.20 m in the case of a very dry summer is also shown in the figure. The presence of a building can be taken into account in a different computer program. The groundwater level under and alongside a terrace of six houses in the near vicinity of a ditch, has been calculated, using this program, see Fig. 3. In all calculations very dry summer conditions have been assumed, for example, such as occurred in 1976.

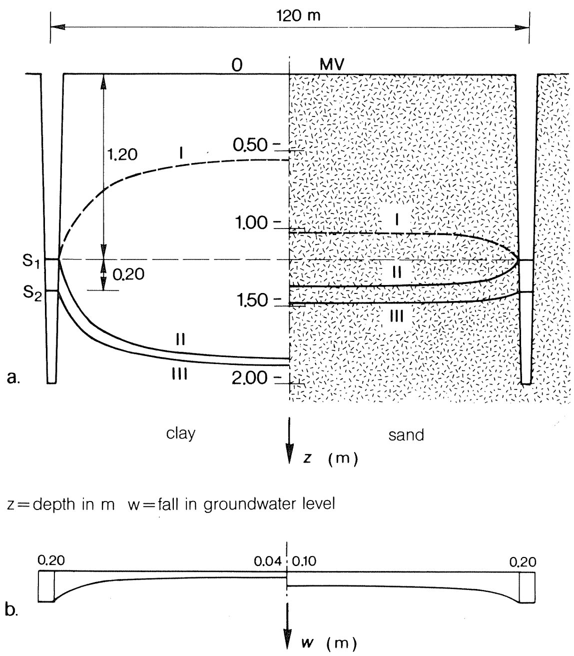

Fig. 2. Groundwater levels in half a parcel for clay (left side) and sand (right side).
a. I. In a wet winter.
II. In a very dry summer.
III. In a very dry summer after a lowering in ditch water level of 0.20 m.
b. The fall in groundwater level in clay and sand.

S_1, S_2 Ditch water level before and after the lowering in surface water level.
MV = groundlevel.

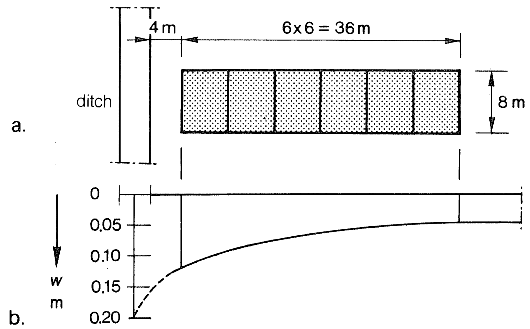

Fig.3.
The average lowest groundwater level under and alongside a terrace of houses near to a ditch.
a. Plan of the terrace showing the position of the ditch.
b. Reduction in groundwater level in a clay subsoil, when the ditch water level is lowered 0.20 m.

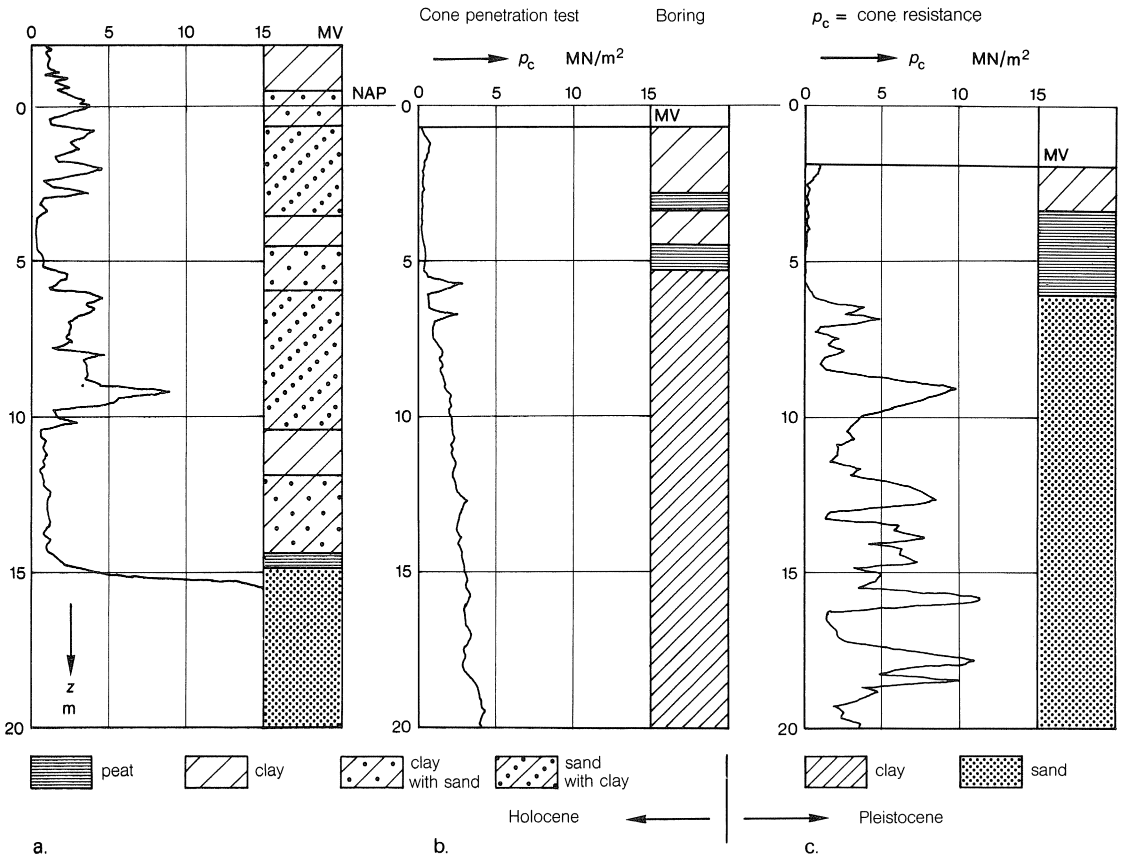

Fig. 4. Results of cone penetration tests and borings for three representative areas of the province.
a. The north: soils consisting mainly of sand.
b. The middle: soils consisting mainly of clay.
c. Around the Eems canal between the cities of Groningen and Delfzijl: soils consisting mainly of peat.
NAP = datum.
MV = groundlevel.

3 Subsoil

3.1 *Constituency of the subsoil*

The shallow subsoil in the area considered developed during the Holocene. The thickness of these subsoil layers is a maximum of 20 m and consists of clay, peat and sand or a combination of these soils. In general these layers are weak; occasionally the sand is somewhat stiffer.

The resistance of successive layers can be determined by means of a cone penetration test. The results of some cone penetration tests for subsoils which are representative of the area are shown in Fig. 4. The same figure also shows the constituency of these subsoils as determined from borings. The relevant properties of the subsoil were determined in the laboratory by oedometer tests and permeability tests on undisturbed soil samples.
Under the layers of the Holocene, there are layers of the Pleistocene, which are very stiff. During the Holocene period the area was flooded by the sea, and a system of creeks

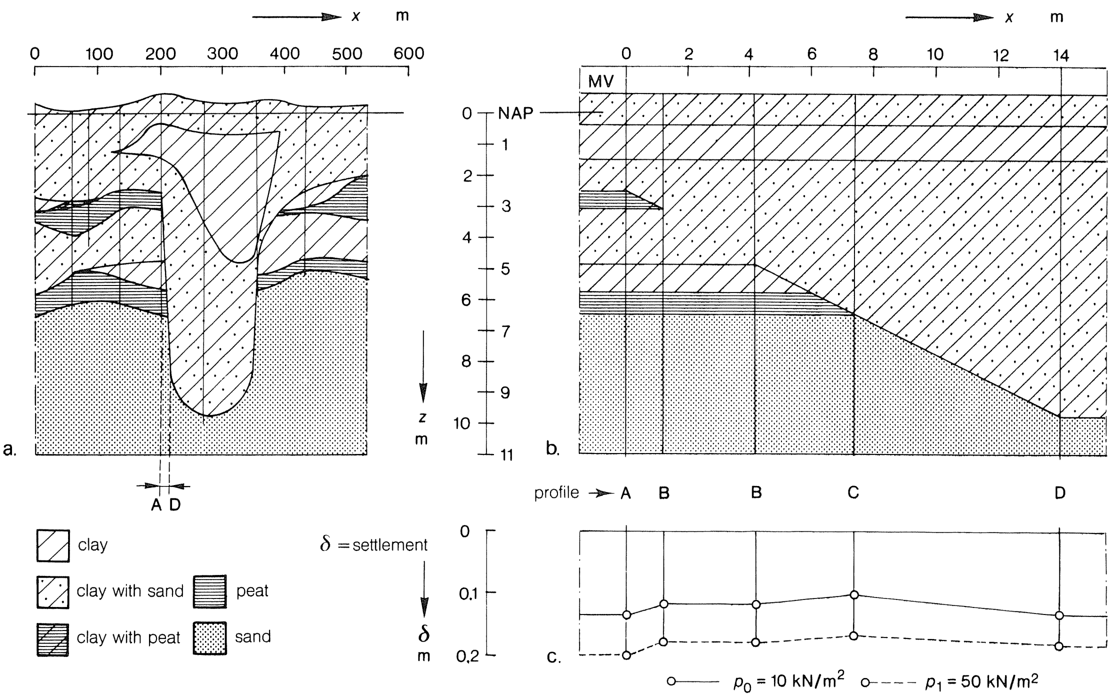

Fig. 5. Inhomogenities of the subsoil.
a. Geological profile in a former creek, near the village of Appingedam.
b. Schematized profile at the left boundary of the former creek indicated in Fig. 5a.
c. Settlements in the vertical Sections A, B, C and D shown in Fig. 5b caused by a uniformly distributed load $p_0 = 10$ kN/m^2 and a one-metre wide strip load $p_1 = 50$ kN/m^2.

was formed in the sandy layers of the Pleistocene. These creek systems were subsequently filled with sea deposits of clay with sand. This is one of the main reasons for the inhomogenities of the Holocene layers, see Fig. 5.

3.2 *Soil mechanics*

Two formulas are used in the Netherlands to determine stresses and deformations of the subsoil. These formulas give reasonably good results for Dutch subsoils.
The stress distribution in the subsoil can be determined by using the Boussinesq formula which describes a radial stress distribution for a single force F on the boundary of a semi-infinite body, see Fig. 6a. The vertical stresses, see Fig. 6b, are given by:

$$\sigma_{zz} = -\frac{3F}{2\pi z^2}\cos^5\theta \qquad (1)$$

A load which is uniformly distributed over a certain area is assumed in Fig. 6b, the point of application of the force F being an imaginary height z_0 above the surface of the subsoil.
The settlements are normally calculated using the Koppejan formula, which combines the load-compression relationship according to Terzaghi and the secular time effect according to Keverling Buisman:

$$\delta = h\left(\frac{1}{C_p} + \frac{1}{C_c}\log t\right)\ln\frac{p+\Delta p}{p} \qquad (2)$$

in which

δ = settlement of a soil layer (m)
h = initial thickness of a soil layer (m)
C_p, C_c = primary and secular compression coefficient
t = time (days)
$p, \Delta p$ = initial load and increment in load (kN/m^2)

The settlement according to Formula (2) is shown in Fig. 7, for a constant load increment as a function of time.

In the area being considered the groundwater level is relatively near to the surface of the subsoil. The influence of the groundwater level on the effective stress is shown in Fig. 8. A fall of the groundwater level causes an increase of the effective stress and has consequently the same effect as the application of a uniformly distributed load. The settlement is then practically proportional to the fall in groundwater level.
When a structure is built on footing foundations, the load will always be distributed. In order to determine the settlements of the building the stresses in the subsoil are first determined in a number of vertical sections, using Formula (1). The settlements in these sections can then be determined with the help of Formula (2). It appears that only the upper few metres of the subsoil are of importance for determining the settlement.

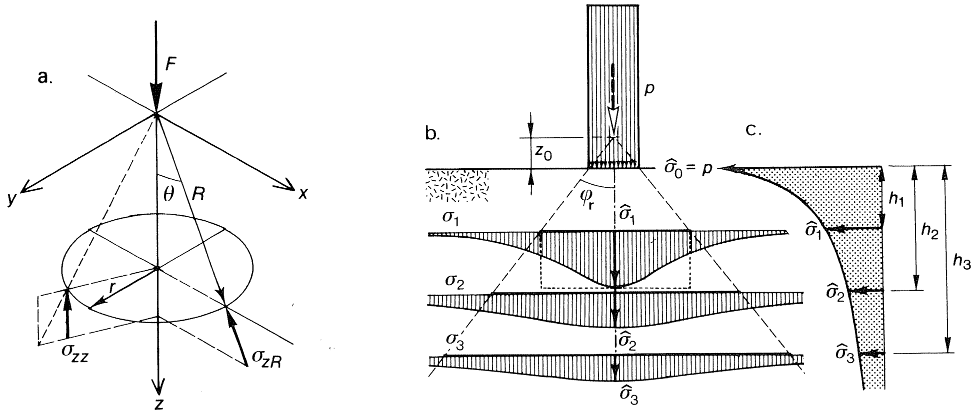

Fig. 6. Radial stress distribution according to Boussinesq.
a. Point load on a semi infinite body.
b. Distribution of the vertical stresses in three horizontal planes.
c. The vertical stress in a vertical section through the centre of the point load.
The dotted lines show the idealized stress distribution according to Section 3.4.

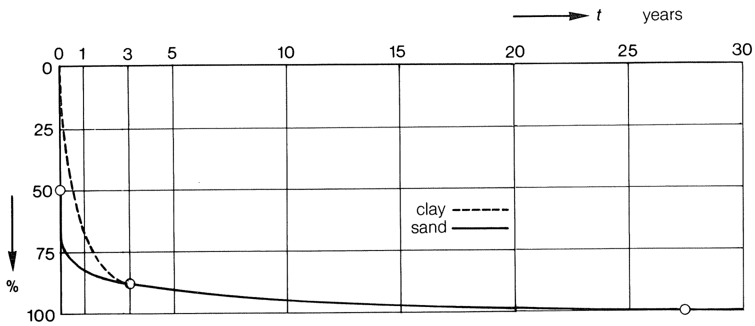

Fig. 7. Settlement as a function of time, due to a quickly applied uniformly distributed load. Settlements are shown as a percentage of the settlements after 30 years.
—— Without groundwater.
------ Influence of groundwater if the subsoil has a low permeability.

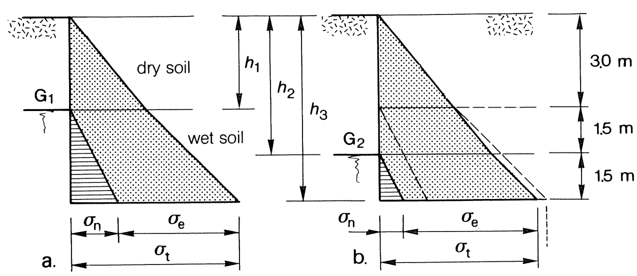

G_1, G_2 Two positions of the groundwater level.

Fig. 8.
Influence of groundwater on stress distribution in the subsoil.
a. Division of the total stresses of the subsoil into neutral stresses and effective stresses.
b. A fall in the groundwater level causes an increase in effective stress.

3.3 *Influence of a pre-load*

In the above it has been assumed that the present stresses in the subsoil have never been exceeded in earlier times. If, in such cases, the loads are relatively low, one can assume that the settlements will be proportional to the increase in load. If the load increment is removed however, a large part of the additional settlement will remain, see Fig. 9. If the load increment is reapplied, the subsoil will resettle to the original loaded level. All changes in load, which are less than the highest load that has ever occurred, will cause the subsoil to behave as a stiff medium. Higher loads however will cause the subsoil to behave as a weak medium.

As mentioned above, a fall in groundwater level may be regarded as the application of a uniformly distributed load. This means that all changes in groundwater level, which are above the lowest level that has ever occurred, will cause the subsoil to behave as a stiff medium. A stiff subsoil reduces the possibility of damage, since it resembles a rigid support.
In a very dry summer, however, the groundwater may reach a level below the lowest that has ever occurred. In this situation the subsoil will behave as a weak medium and in some cases this might lead to cracking in masonry buildings. This is assumed to be the reason for numerous reports of damage after some very dry summers.

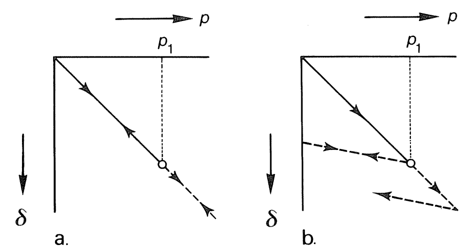

Fig. 9. Load - deflection diagrams when time effects are neglected.
a. Elastic material.
b. Subsoil (schematized).
The steep section in Fig. 9b is only valid for increasing loads which have not been previously applied. For all other loading possibilities the more gently sloping sections are valid; two such sections are shown in the figure.

3.4 *Schematization of subsoil properties*

In order to determine the interaction between structure and subsoil, the properties of the subsoil have to be schematized, so that they can be fitted into normal building calculations [2, 3]. Initially the subsoil is regarded as a homogeneous, isotropic and elastic medium. A layer of subsoil with a height h and a modulus of elasticity E is now assumed, which is supported by a completely rigid sublayer.

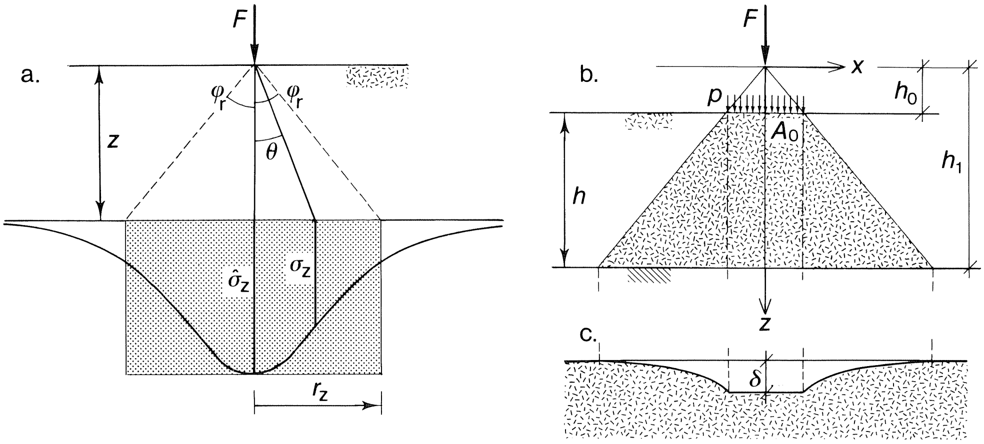

Fig. 10. Schematization of the stress distribution.
a. Introduction of a circular equivalent area with radius r_z.
b. Cone-shaped body in which all deformations are assumed to take place.
c. Deflections under and alongside the loaded area.

The stress distribution, which is shown in Fig. 6, is now replaced by an equivalent distribution, uniformly distributed over a circular area, which, at each height, has the same stress in the z-axis as the original stress distribution, see Fig. 10a. In this way a cone is defined, in which all deformations are assumed to take place, see Fig. 10b.
To avoid infinitely high stresses (and settlements) under the point of application of the load, the cone is truncated. The surface of the subsoil is then uniformly loaded over a circular area A_0. The vertical displacement of the area A_0 is then equal to:

$$\delta = \frac{F}{EA_0} \frac{h_0}{h_1} h \tag{3}$$

To simplify the calculations, the circular area is replaced by an equivalent square area, which is defined by tan $\varphi = 2h_0/d_0 = 1.38$, see Fig. 11a.
The same angle is adopted in the case of strip loading, see Fig. 11b. The vertical displacement of the area A_0 is then equal to:

$$\delta' = \frac{Fh_0}{EA_0} \ln\left(1 + \frac{h}{h_0}\right) \tag{4}$$

If the surface of the subsoil is subjected to a uniformly distributed load, the totale load $\bar{F}$ on the area A_0 will be supported by the prism under this area, see Fig. 11c. The vertical displacement of the surface of the subsoil is then equal to:

$$\bar{\delta} = \frac{\bar{F}h}{EA_0} \tag{5}$$

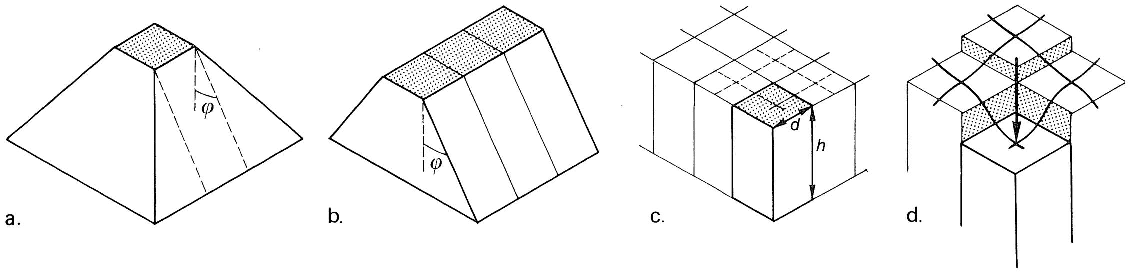

Fig. 11. Schematization of the subsoil.
a. Load distribution in the form of a truncated pyramid.
b. Load distribution for strip loading.
c. Subdivision of the subsoil into prisms.
d. Connection of the individual prisms by coupling beams in the x and y-directions.

From the assumptions in the calculations, all areas A_0 will undergo a rigid vertical displacement.
If the displacement $\bar{\delta}$ from Formula (5) is made equal to the displacement δ from Formula (3), the ratio $\bar{F}/F$ indicates that part of the load on the area A_0, which is supported by the prism under the load. The remainder of the load is supported by the surrounding subsoil. The ratio $\bar{F}/F$ is equal to:

$$\bar{F}/F = h_0/h_1 = \beta \cot \varphi/(\beta \cot \varphi + 2) \tag{6}$$

in which $\beta = d_0/h$, see Fig. 12a.

3.5 *Replacing the subsoil by a system of coupled springs*

The subsoil is divided into prisms, each having a height h and a square ground surface with a side d, see Fig. 11c. These prisms are regarded as a system of springs, which are mutually coupled. If one such spring is loaded and deflects, the adjacent springs are also deflected and take over a part of the load, see Fig. 11d.
The load ΔF which is transmitted between two adjacent springs, is assumed to be proportional to the difference in vertical displacement between these springs, see Figs. 12b and 12d:

$$\Delta F = k_1(\delta_0 - \delta_1) \tag{7}$$

The "spring constant" of one prism k_0 follows from Formula (5) and is equal to:

$$F = \frac{EA_0}{h}\,\delta_0 = k_0\delta_0 \tag{8}$$

To fulfil the condition indicated by Formula (7), the prisms are interconnected by coupling beams with a certain bending stiffness and no torsional stiffness. These coupling beams are free to deflect but they are not allowed to rotate at the centres of the springs, see Fig. 12e.

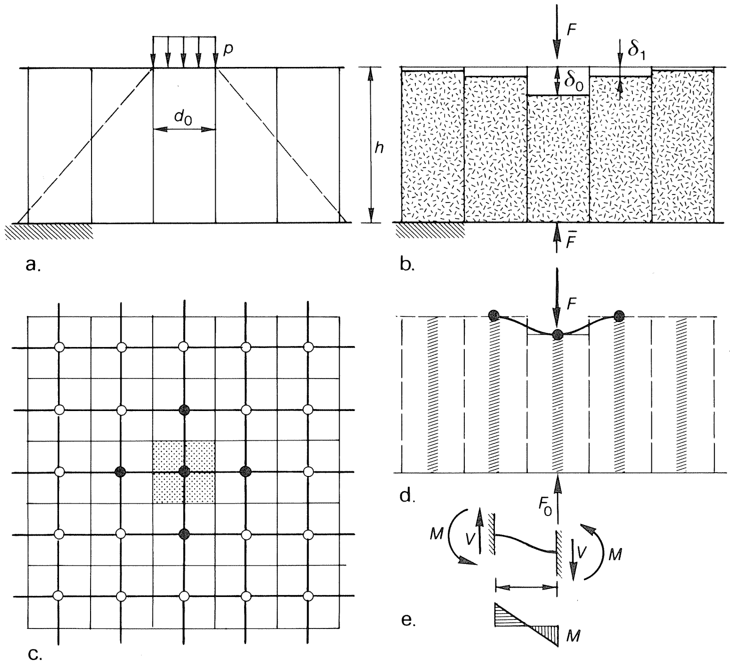

Fig. 12. Subsoil considered as a system of coupled springs.
a. Subdivision of the subsoil into prisms.
b. The loaded prism transfers a part of the load to surrounding prisms.
c. Top view of prisms with coupling beams.
d. Determination of the constant k_1.
e. s-shaped deflection of the coupling beams.

The bending stiffnesses of the springs must now be chosen in such a way, that the original load distribution according to Boussinesq, is approximated as correctly as possible. In other words: the condition indicated by Formula (6) has to be satisfied. To achieve this, a number of computer calculations have been carried out for a grid as shown in Fig. 12c, where only the central spring has been loaded. In these calculations the bending stiffness of the coupling beams has been varied in relation to the stiffnesses of the individual springs. The part of the central load supported by the central spring and the part which is transferred to the surrounding springs follow from these calculations. As a result of the calculations the ratio $\bar{F}/F$ can be expressed as a function of $\mu_1 = k_1/(k_0 + 4k_1)$.
At the same time the ratio $\bar{F}/F$ must be as indicated in Formula (6). A relationship between μ and $\beta = d/h$ can be obtained by a graphical solution, see Fig. 13.
From Fig. 13 it follows that, for $\beta \leqq 0.75$, the following linear relationship will give a good approximation:

$$\mu_0 = 0.40\beta \qquad \mu_1 = \frac{1}{4}(1 - \mu_0) = 0.25 - 0.10\beta \tag{9}$$

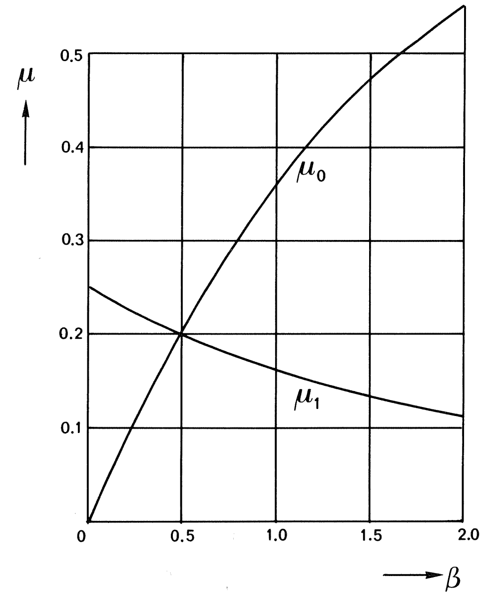

Fig. 13. Redistribution coefficients μ_0 and μ_1 as a function of $\beta = d/h$.

In order to check the validity of the results, a two-dimensional problem has been solved, using the coupled springs schematization of the subsoil. The results have been compared with the well known solution of the diametrically loaded disc, which is based on the Boussinesq formula for two-dimensional radial stress distribution. This solution in its turn, resembles fairly well the case of a single load on a layer which is supported by an infinitely stiff sublayer. As can be seen from Fig. 14, the agreement is quite satisfactory.

3.6 *Calibration of subsoil settlement calculations*

The settlements of the subsoil in the area being considered, have been predicted in the way described in Section 3.2, using a computer program. A typical subsoil profile is shown in Fig. 15a. The calculations have been carried out for a number of uniformly distributed loads on footing foundations of various widths. Some results are shown in Fig. 15b and it is obvious that the settlement of a footing of a given width is practically proportional to the load.

Similar calculations have been carried out for a homogeneous subsoil schematized according to Section 3.4, using Formulas (4) and (5). The width b of the footings and the height h of the subsoil have been considered to be variables. In all cases the ratio between the settlements of the footings and the settlement of the subsoil has been determined assuming that the same continuously distributed load which is applied to the strip is also applied over the full area ($b = \infty$). This ratio Φ is independent of the magnitude of the load and has been plotted in Fig. 15c as a function of b and h.

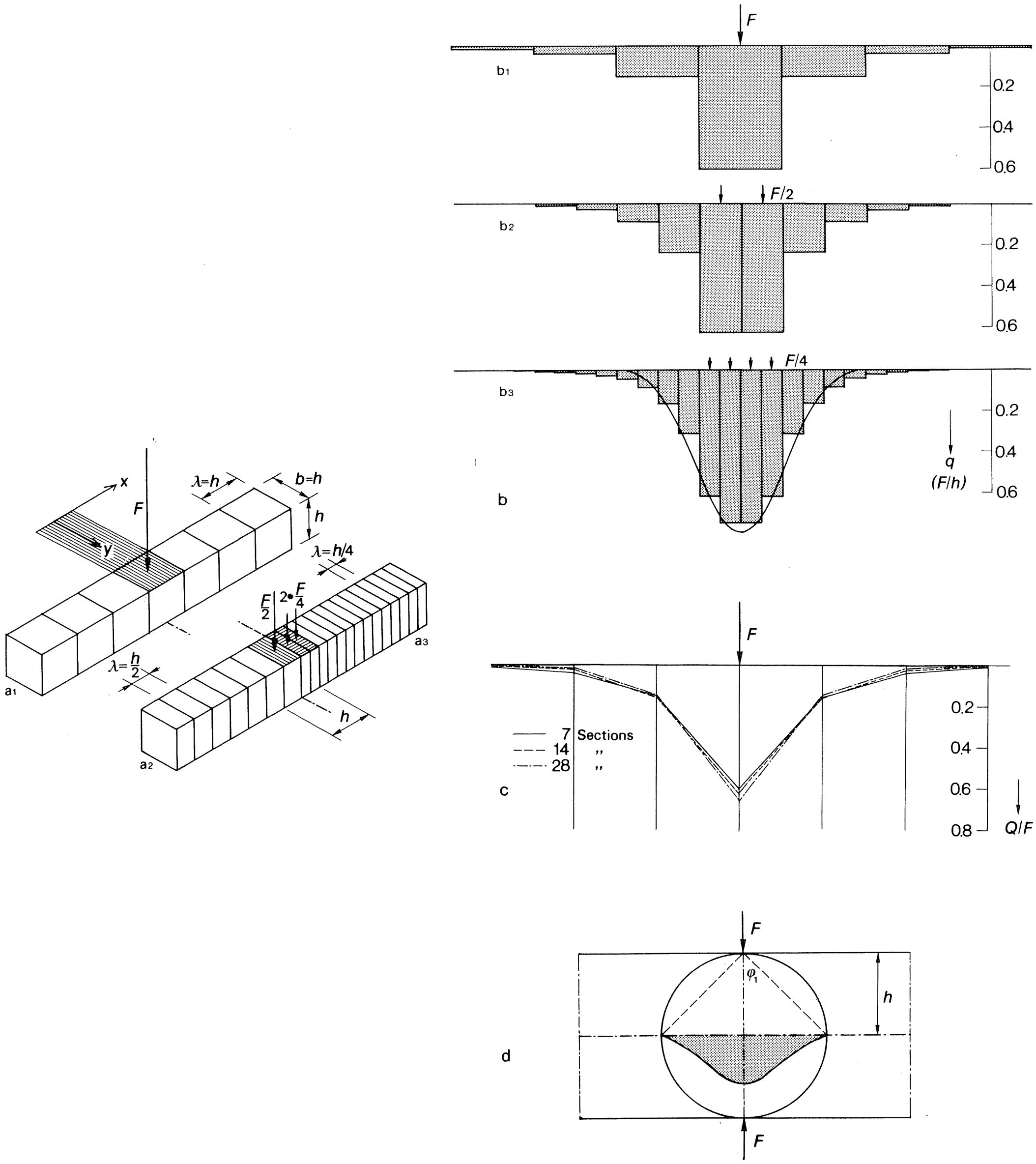

Fig. 14. Check of the validity of the system of coupled springs.
a. Strip loading in y direction of a layer of soil with a thickness h. Calculation of a groundstrip in x direction, in which the groundsurfaces of the successive springs successively have been reduced.
b. Counter pressure per unit length for the three cases being considered.
c. Total counter pressure for prisms with a square area of $h \times h$.
d. Vertical stress distribution along the x-axis for a diametrically loaded disc. The superposition of four of these loads is shown in Fig. $14b_3$.

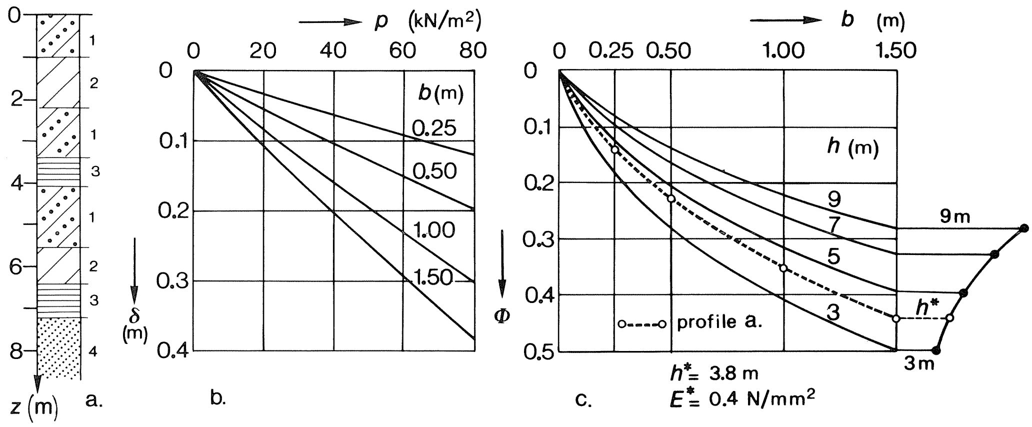

Fig. 15. Calibration of subsoil settlement calculations.
a. Representative profile of the subsoil.
1=sandy clay, 2=clay, 3=peat, 4=Pleistocene sand.
b. Settlement of a number of strip footings as a function of the strip width and the load; application of Formulas (1) and (2) for the profile given in Fig. 15a.
c. ratio Φ for various layer thickness.
—— Elastic calculation according to Formula (4).
------ Profile of the subsoil given in Fig. 15a.

The same ratio Φ has also been determined for the real subsoil and is shown in Fig. 15c as a dotted line. It is obvious that the shape of this settlement curve closely agrees with the shape of the curves for the schematized subsoil. The effective height h^* of the schematized subsoil is then easily determined graphically, see Fig. 15c (to the right), from which follows the magnitude of the effective modulus of elasticity E^*. Both quantities are then used to replace the real subsoil by a system of coupled springs, as described in Section 3.5. This procedure can always be applied, as only the settlement at the base of the footing foundation has to be the same for both the real and schematized subsoil.

4 Stress distribution in a building

4.1 *Stress distribution in a "basic unit"*

When calculating the stress distribution in a building which has a supporting structure of steel or reinforced concrete, it is customary to divide the building into a series of bays, and to calculate each bay as a two-dimensional frame work. Masonry buildings however, generally do not have a true supporting structure, consisting of a material which possesses plastic qualities, which is necessary for a limit design.
Masonry is a stiff but brittle material which is able to transmit rather large compressive stresses. Relatively much smaller tensile stresses however, cause cracking.

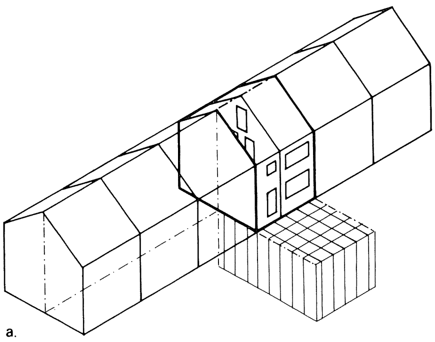

Fig. 16.
A terrace of six houses.
a. The “basic unit” is supported by a system of coupled springs. The adjacent houses are assumed to undergo the same stress distribution as the house being considered.
b, c, d. Subdivision of the walls into finite elements.
b. Floor supporting wall.
c. Intermediate wall.
d. Front and rear wall.

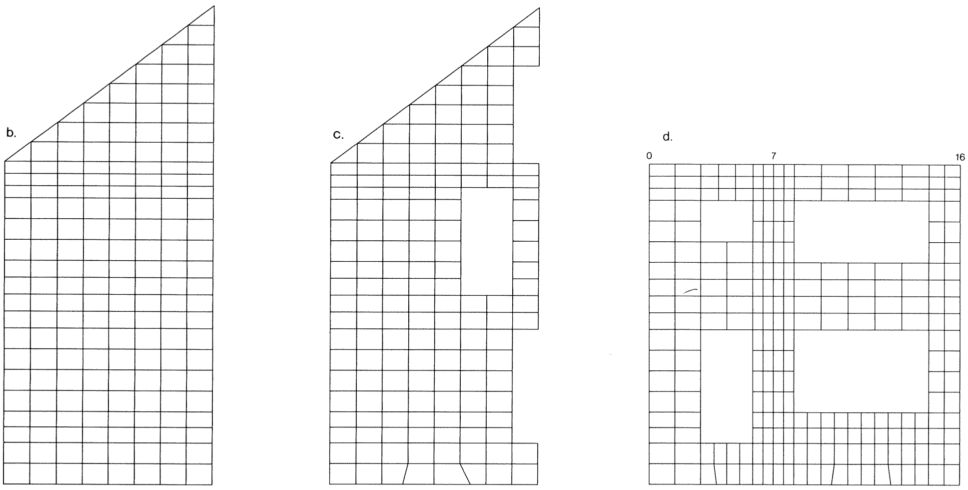

Even if masonry is regarded as an elastic, homogeneous and isotropic or orthotropic material, calculations are still difficult since houses consist of a composition of plates with and without openings, basically loaded “in-plane”. Floors, walls and foundation form a three-dimensional configuration and calculations basically have to be carried out by means of computer programs, using the finite element method.
To reduce the amount of calculation, one house of the terrace is regarded as a “basic unit”, see Fig. 16a. In this basic unit the complicated stress distribution in the walls of the building and the interaction with the subsoil are taken into account. The other houses of the terrace are assumed to be in exactly the same position as the basic unit. The influence of the finite length of the terrace of houses is subsequently taken into account, considering the terrace as an equivalent “beam”.
The walls of the basic unit are divided into finite elements, see Fig. 16. With the help of a computer program, the stresses in the walls can be calculated. If the houses have a foundation consisting of concrete piles, these can be regarded as rigid supports, and the calculations can be carried out in the usual way.

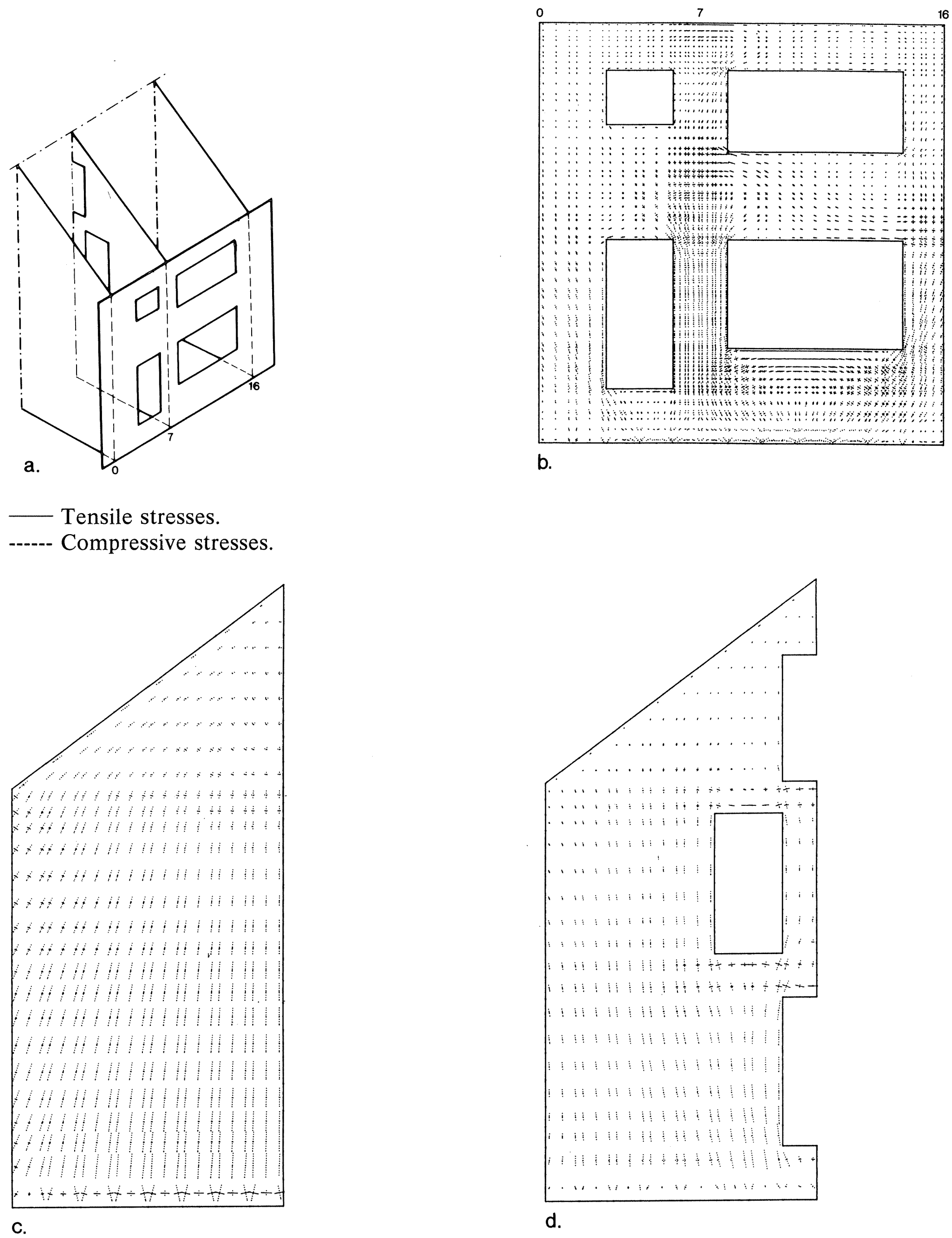

Fig. 17. Stress distribution in the walls of a basic unit, due to the direct transfer of the dead weight to the subsoil (system of coupled springs).
The magnitude and direction of the principal stresses are shown in the figures.
a. Geometry of the finite element model.
b. Front and rear wall.
c. Floor supporting wall.
d. Intermediate wall.

If a footing foundation is applied however, the walls are directly connected to the weak subsoil via the footings. It is therefore necessary to consider a series of soil prisms under and alongside the basic unit, see Fig. 16a. For the calculation these prisms are considered as a grid on an elastic foundation, see Figs. 12c and 12d.
Calculations have been made using the DIANA computer program. The results are given in Fig. 17, as the magnitude and direction of principal stresses in the walls. Since the building is very stiff compared with the subsoil, the stress distribution in a building on footing foundations is quite different to one founded on rigid supports.
The basic unit undergoes a vertical displacement more or less like a rigid block. Due to the load distribution and the relatively small influence of the various widths of the strip footings, the counter pressures of the various walls are more or less similar. The direct loads from the various walls differ strongly however. The side walls which support the floors are heavily loaded in comparison with the front and rear walls. Equilibrium has to be restored by shear stresses between these walls, as shown in Fig. 18.
In the traditional approach, shown in Fig. 19, the width of the footings is chosen such, that the counter pressure under all footings is the same and only related to the direct transfer of dead weight to each footing. In this approach the subsoil is regarded as a system of uncoupled springs, whereas it was argued above, that the subsoil should be regarded as a system of coupled springs. In reality therefore the counter pressure can differ considerably from that shown in Fig. 19.
From the calculations it also follows, that the stiffness of the subsoil can vary between wide limits, before the stress distribution in the walls is even slightly affected.

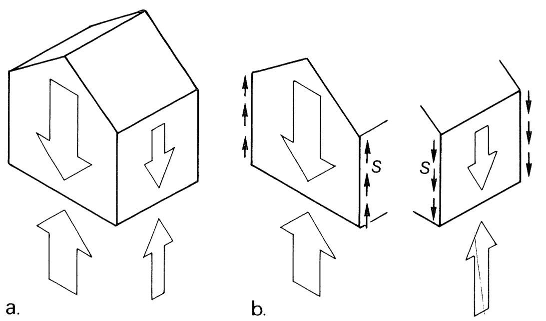

Fig. 18.
Transfer of the load if the subsoil is considered as a system of coupled springs.
a. The dead weight of the walls and the counter pressure from the subsoil, shown schematically.
b. Equilibrium has to be restored by shear forces, S, acting at the connection between two perpendicular walls.

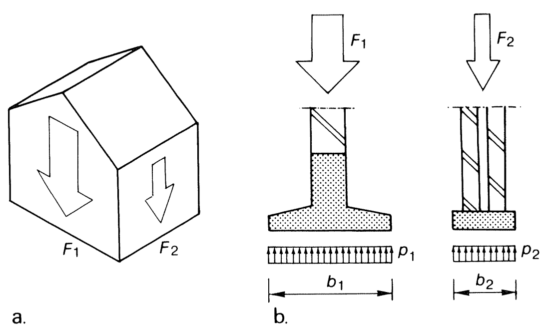

Fig. 19.
Standard determination of the width of a strip footing if the subsoil is considered as a system of uncoupled springs.
a. The dead weight of the walls, shown schematically.
b. Determination of the width of the strip footings; if $b_1/b_2 = F_1/F_2$, the counter pressures under both footing strips will be equal and therefore $p_1 = p_2$.

4.2 *Stress distribution in a terrace of houses*

The stress distribution becomes somewhat different if a terrace of houses is considered instead of one single basic unit. The reason of this difference is shown in Fig. 20. All the intermediate houses of the terrace are supported to a certain extent by the subsoil along the front and rear wall of each house. The houses at both ends of the terrace are, in addition, also supported by the subsoil along the end walls. The major part of the dead weight is still directly transferred to the subsoil, as shown in Fig. 21b. However due to the stiffness of the terrace, a small percentage of the dead weight of the terrace is transported to the end walls, see Fig. 21c. For this part of the load the terrace of houses acts more or less as a simply supported beam, see Fig. 21d.
The bending moments and shear forces in such an elementary beam are shown in Fig. 22. For convenience all loads are concentrated at the floor bearing walls. For the calcu-

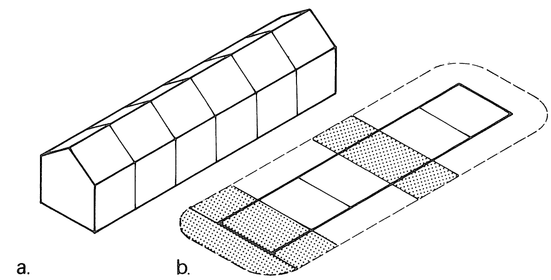

Fig. 20.
The effect of end houses on the loads on a terrace of six houses.
a. Terrace in perspective.
b. Difference between the support from the subsoil for an end house and a house in the middle of the terrace.

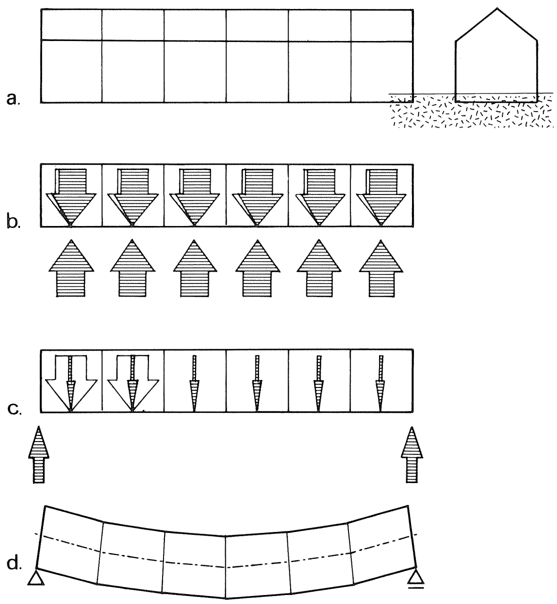

Fig. 21.
Division of the load of a terrace of six houses.
a. Side and front view of the terrace.
b. The major part of the dead weight is supported directly by the subsoil.
c. A small part of the load is supported by the end walls as for a simply supported beam.
d. The shape of the deflected "equivalent beam", shown schematically. Each house is regarded as one element of this beam.

lations it is essential that the bending moment for each basic unit is split into a constant part and a linearly varying part as shown in Fig. 22d for the second basic unit from the right.

The "beam" itself consists of the front and rear walls of the terrace. Any possible contribution of the floors, as flanges of the "beam", is not taken into account. The stress distribution in a beam with openings "in the web" however, is more complicated than in a beam without openings.

When calculating the stress distribution in the terrace of houses, it is very useful to determine initially, in an elementary way, the stress distribution in an equivalent beam on an elastic foundation, consisting of coupled springs. These calculations indicate which part of the dead weight is directly transmitted to the subsoil and which part is transmitted via bending moments to the end walls, see Figs. 21b and 21c.

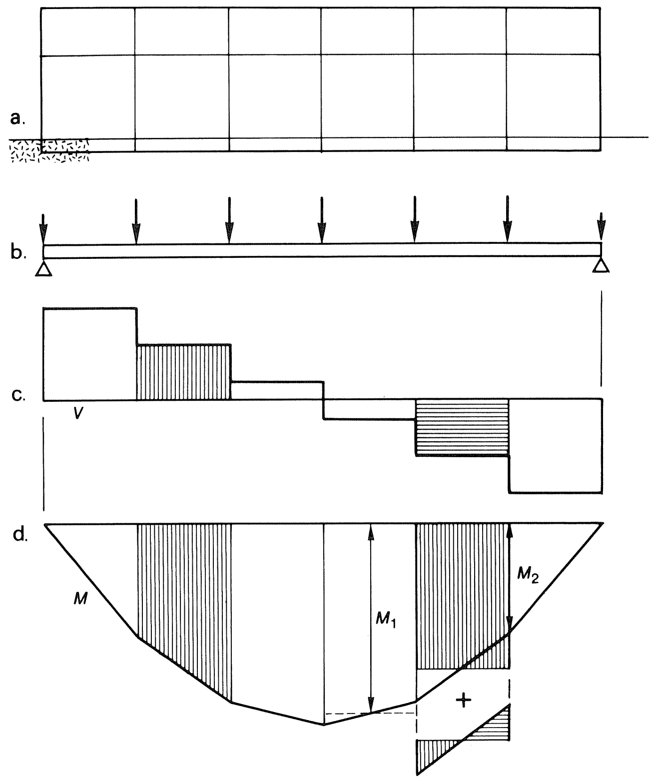

Fig. 22. Stress distribution for a terrace of houses, in which a small part of the load is transferred to the end walls.
a. Front view of the terrace.
b. An "equivalent beam" with the dead weight concentrated at the floor bearing walls.
c. Shear force line.
d. Bending moment line; at the second house from the right, the bending moment has been divided into a constant moment and a moment which varies linearly.

The results for the transmission of a small part of the dead weight as a beam to its supports can be presented as curves for the shear force and the bending moment. In this sort of calculation, the variables which govern the problem, can easily be varied. The detailed stress distribution in the walls, has then only to be determined for representative loading cases.

The stress distribution in the equivalent beam is also determined using the finite element method. For this calculation the bending stiffness and the shear stiffness of the equivalent beam have to be known. To determine these parameters the terrace of houses is divided into coarse elements each consisting of one basic unit, see Fig. 21d. Fig. 23 shows the various loading cases to which such an element is subjected. The direct transfer of the load to the subsoil is shown in Fig. 23a, taking into account the transmission of shear forces, as shown in Fig. 18b. The constant bending moment is shown in Fig. 23b and the linearly varying bending moment (constant shear) in Fig. 23c. All three basic loading cases shown in Fig. 23 are applied to the three-dimensional model of the basic unit. The stress distribution due to the direct transfer of dead weight to the subsoil has already been shown in Fig. 17. For the two other loading cases, a stress distribution has been applied at both ends of the front and rear wall of the basic unit. This stress distribution has been determined in an elementary way for the case of a constant bending moment. This bending moment has been applied at Section B-B shown in Fig. 23b, assuming that plane cross-sections remain plane, see Fig. 23d.

In the loading case, shown in Fig. 23c, both moments have the same direction of rotation and the required counter pressures are supplied by the springs of the foundation.

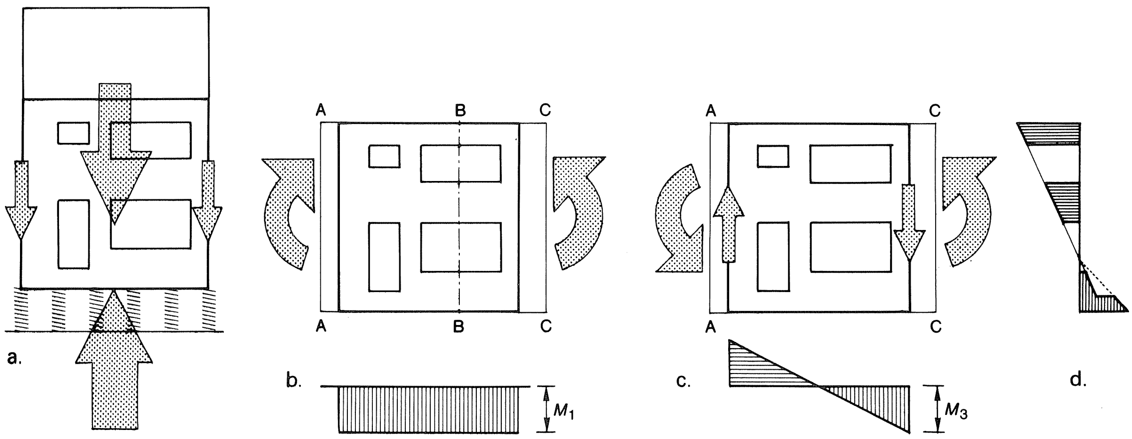

Fig. 23. The load transfer mechanism for one basic unit of the terrace.
a. Direct transfer of the load to the subsoil (loading Case 3).
b. Constant bending moment (loading Case 1).
c. Linearly varying bending moment (constant shear) (loading Case 2).
d. Stress distribution at Cross-section B-B Fig. 23b, assuming that plane cross-sections remain plane. This same stress distribution has also been applied to Cross-sections A-A and C-C see Fig. 23b and c.

The principal stresses and the deformations for the constant bending moment are shown in Fig. 24 and for the linearly varying moment in Fig. 25. The bending stiffness and the shear stiffness of an element of the equivalent beam are easily determined from these deformations.

Fig. 24 indicates that the stress distribution and the deformations are in good agreement with those of an elementary beam; the stress distribution varies more or less

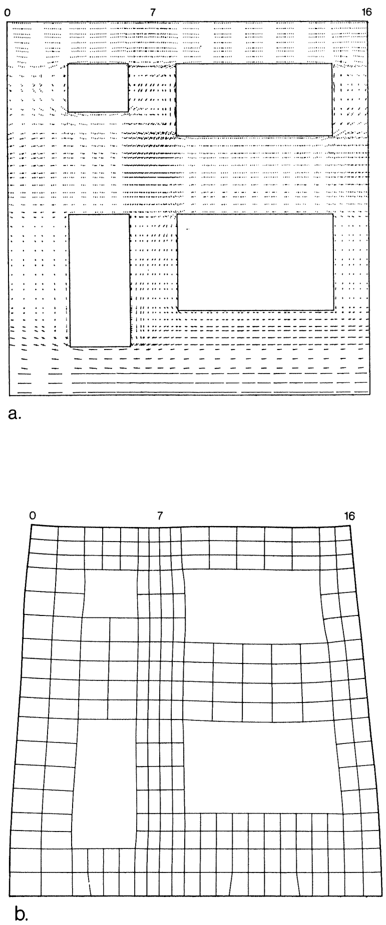

Fig. 24.
Constant bending moment in a front or rear wall, see Fig. 23b ($M_1 = 600$ kNm).
a. Magnitude and direction of principal stresses.
b. Deformations - highly exaggerated. (Modulus of elasticity of masonry (walls) and concrete (foundation): $E_m = 6000$ N/mm^2, $E_c = 12000$ N/mm^2).

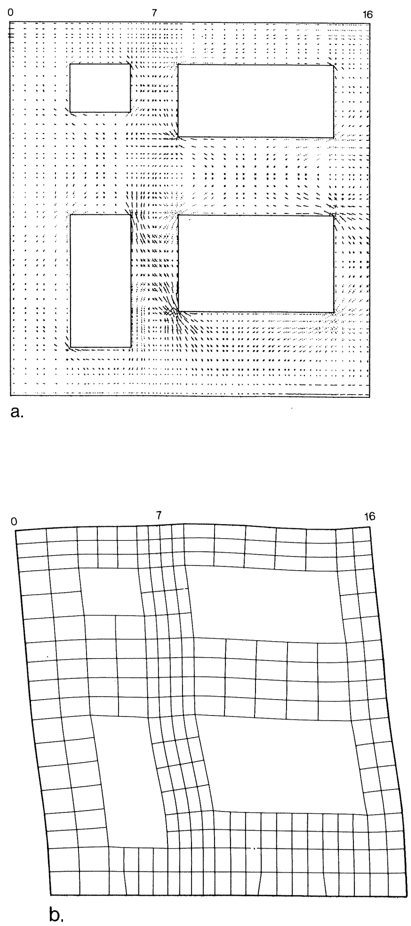

Fig. 25.
Linearly varying bending moment in a front or rear wall, see Fig. 23c ($M_3 = 600$ kNm, shear force $V =$ constant).
a. Magnitude and direction of principal stresses.
b. Deformations - highly exaggerated.

linearly and plane sections remain more or less plane. If a constant shear force has to be transmitted, however, the stress and deformation patterns differ considerably from that given by elementary theory. In this case the shear force deformation is composed of the bending deformations of the parts of the wall between the door and window openings and high peak stresses are to be expected especially in the corners of these openings, see Fig. 25a.
Finally the elastic support given by a system of coupled springs has to be adapted to the calculation as an equivalent beam. This is rather simple since the terrace of houses is displaced more or less vertically as a rigid block. The houses themselves are now neglected and only the system of strip footings is considered, see Fig. 26b. This system of strip footings is now given a rigid vertical displacement and the subsequent settlement of the subsoil, regarded as a grid of beams, is determined using a computer program for grids, see Fig. 26a. This calculation gives the transmitted forces between the footing and the adjacent subsoil due to the imposed vertical displacement. Therefore the "spring stiffness" per unit length can be determined for each part of the strip footing. In this way the springs under the equivalent beam can be considered as uncoupled springs, because the mutual interaction between the subsoil springs has already been taken into account in the calculation procedure.

4.3 *Homogeneous subsoil*

In the most ideal situation the subsoil is completely homogeneous and calculations will only show the influence of the geometry of the buildings. For the terrace of houses a building type has been chosen that can be regarded as representative for the area con-

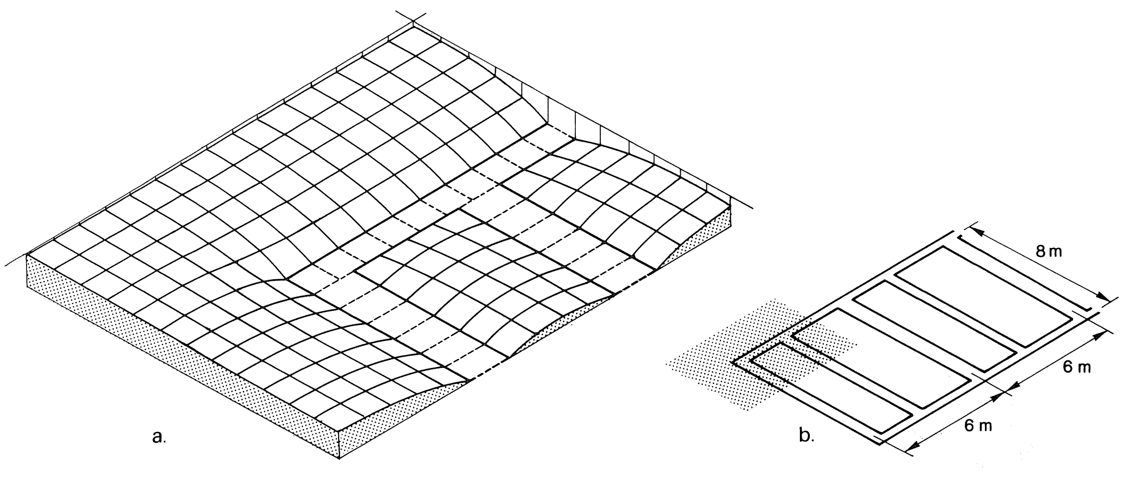

Fig. 26. Deflections of the subsoil if a rigid displacement is given to the strip footings.
a. Vertical displacement of the subsoil.
b. Plan of the strip footings of two houses at the left end of the terraces. The section of the subsoil shown in Fig. 26a has been shaded in Fig. 26b.

sidered. Cross-sections and plan are shown in Figs. 27a and 27b. The equivalent beam with its loads and the supporting springs are shown in Fig. 27c. Large point loads act on the equivalent beam at the location of the floor bearing walls. At the same time the related equivalent spring stiffnesses are also much higher than between these walls, due to the length of these transverse walls.
The bending moment due to dead weight is shown in Fig. 28a. For the second house from the right the bending moment is split into three parts:

1. A constant bending moment, with a stress distribution as shown in Fig. 24a.
2. A linearly varying bending moment, with a stress distribution as shown in Fig. 25a.
3. A more or less parabolic negative bending moment, due to the direct transfer of the load to the subsoil, which causes a redistribution of the load between the transverse and the longitudinal walls. The related stress distribution is shown in Fig. 17b.

The final stress distribution in each terrace house can now be obtained by multiplying all stresses of each loading case by an appropriate factor and superimposing them. Obviously this is done with the help of a computer program. It has been found to be sufficient to do this only for one house in the middle of the terrace and one at the end.
The moments resulting from changes in groundwater level are shown in Fig. 28b. The terrace of houses is situated unfavourably in all cases because it is near a ditch, as shown in Fig. 3, for a subsoil consisting of clay, where variations in the groundwater level have to be expected as shown in Fig. 2 at the left.

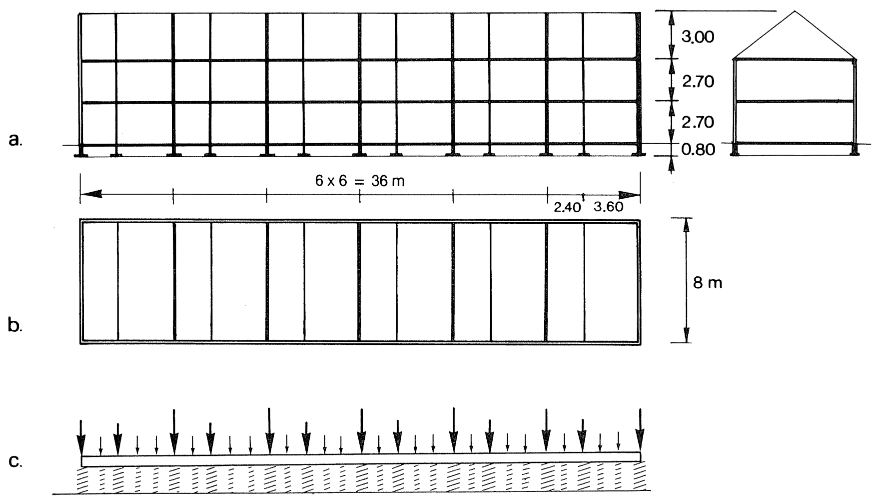

Fig. 27. Terrace of six houses, considerd as a beam on elastic foundation (spring stiffnesses adapted).
a. Longitudinal and transverse cross-sections.
b. Plan.
c. Distribution of loads and spring stiffnesses.

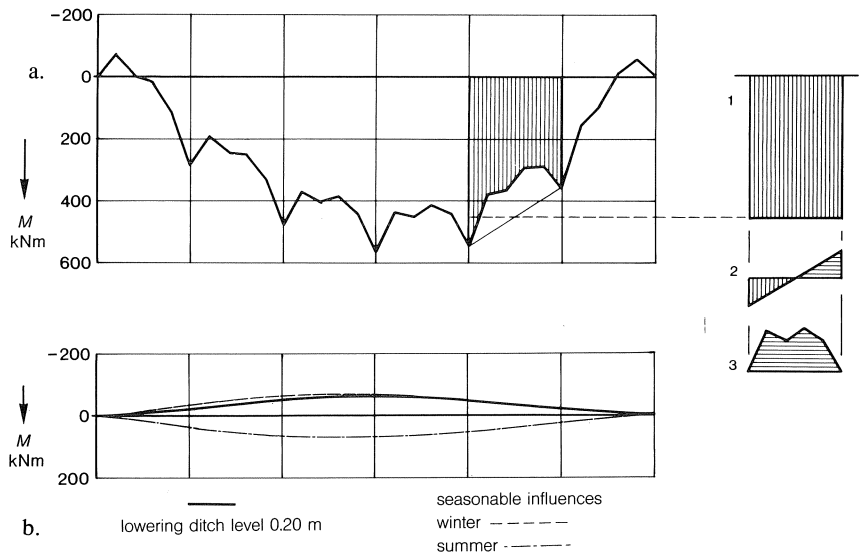

Fig. 28. Bending moments in the terrace of Fig. 27. The bending moments refer to a subsoil which consists mainly of clay.

a. Bending moments due to the dead weight of the terrace and a division of the bending moment into three parts for the second house from the right.

b. Bending moments due to a lowering in water level of 0.20 m in a ditch near to the terrace and bending moments due to seasonal influences.

The moments are shown for a rise and fall of the groundwater around a neutral position (=level of water of the ditch) caused by extreme seasonal influences. In this case the subsoil will act as a stiff medium. The effect of a fall in groundwater level, caused by the water level in the ditch being lowered 0.20 m below the lowest level ever reached before, is also shown in Fig. 28b. In this case the subsoil will act as a weak medium. It is obvious that for the cases considered the numerical value of the bending moment is almost the same. A fall in groundwater level will always give a hogging effect to the settlements of the subsoil and a negative bending moment is produced over the whole length of the terrace, with however, a rather low numerical value.

4.4 *Inhomogeneous subsoil*

As mentioned in Section 4.3 a fall in groundwater level will produce negative bending moments in the terrace of houses, if this is situated perpendicular to a ditch in the near vicinity. This has a relieving influence on the positive bending moments due to the transfer of the dead weight. Because this will not have adverse effects on the terrace, this situation has not been investigated further for the case of an inhomogeneous subsoil.

Towards the middle of a parcel the groundwater falls to a more or less constant level, see Fig. 2. Due to inhomogenities of the subsoil, however, a constant fall of the groundwater level may still lead to variable subsoil settlements.

In order to find out more about this effect, an example has been considered in which there is a variation in the subsoil composition as indicated by a group of nearby borings. The variation in soil composition found at the edge of a creek, see Fig. 5a, has been schematized in Fig. 5b.

By using Formulas (1) and (2) the settlements have been determined for two loading cases: a strip loading for a width of 1 m ($p = 10$ kN/m^2) and a uniformly distributed load ($p = 50$ kN/m^2). Both settlement curves are shown in Fig. 5c. These settlements can be converted into curves for the variation of the modulus of elasticity of the subsoil, see Figs. 29b and 29c. The differences between the values for strip loading and a continuously distributed load are due to the fact that in the second case the deeper laying layers have a greater influence than in the first case.

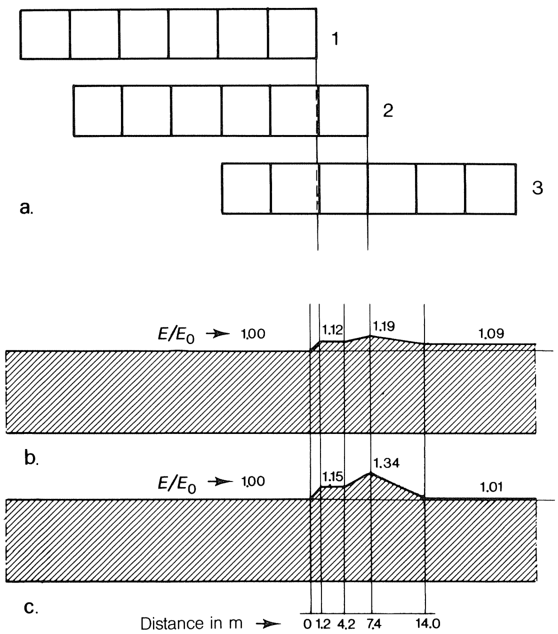

Fig. 29. Variation in the equivalent modulus of elasticity for an inhomogeneous subsoil according to Fig. 5b.
a. The terrace of six houses, in three different locations, relative to subsoil inhomogeneity.
b, c. Stiffness of the subsoil, expressed as the ratio of the moduli of elasticity of the inhomogeneous and the homogeneous subsoil.
b. The subsoil stiffness ratio for the dead weight of the terrace.
c. The subsoil stiffness ratio for a fall in groundwater level.

As a theoretical experiment the terrace of houses has been shifted in a longitudinal direction towards the inhomogenities of the subsoil, see Fig. 29a and the bending moments due to dead weight have been determined for three positions, see Fig. 30. The variation of the modulus of elasticity has been taken as that shown in Fig. 29b.

In Position 1 the right hand end wall is supported by the stiffer section of the subsoil. The increase in bending moment, compared with the case of a homogeneous subsoil, Fig. 28a, is rather small. In Position 2 however, the last basic unit is completely supported by the stiffer section and the bending moments become more than twice as large as in the case of the homogeneous subsoil.
In Position 3 the middle of the terrace is completely supported by the stiffer section. The bending moments are now greatly reduced, because the extra supporting effect of the end walls becomes relatively smaller.
The bending moments for a uniform fall in groundwater level of 0.20 m is shown in Fig. 30b for the same three positions. In this case a variation of the modulus of elasticity according to Fig. 29c has been assumed. For Positions 1 and 2 the bending moments are

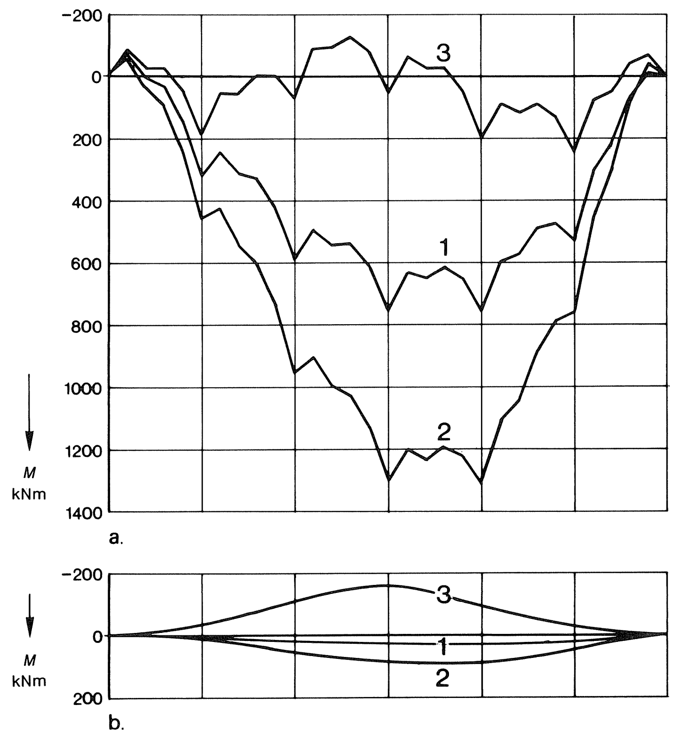

Fig. 30. Bending moments for the terrace of six houses on inhomogeneous subsoil, located at the three positions indicated in Fig. 29a.
a. Bending moments due to dead weight.
b. Bending moments for a uniform fall in groundwater level of 0.20 m.

relatively small, but in Position 3 they are somewhat larger. Position 3 is relatively unfavourable because negative bending moments occur in the terrace due to dead weight alone.

4.5 *Influence of strip width*

In the above the geometry of the terrace and the qualities of the subsoil were assumed to be known. Often however, if the possibility of damage to existing terraces has to be investigated, the geometry of the foundation is unknown and its influence on the stress distribution must be investigated in more detail.
As mentioned before, only footing foundations need to be considered since these are the most vulnerable to a fall in groundwater level. From the calculations it follows especially that the difference in the width of the various parts of the footings has a major influence on the bending moment in the equivalent beam.
Some possible configurations of footing widths are shown in Fig. 31b. The bending moments for these configurations are shown in Fig. 31a. This figure has been simplified by omitting the parabolic parts of the bending moment diagram.
A reduction of the width of all (equal) footings has a relatively small influence, compare Case A-1 and A-3. This agrees with the fact mentioned above that the absolute value of the stiffness (modulus of elasticity) of the subsoil has a relatively small

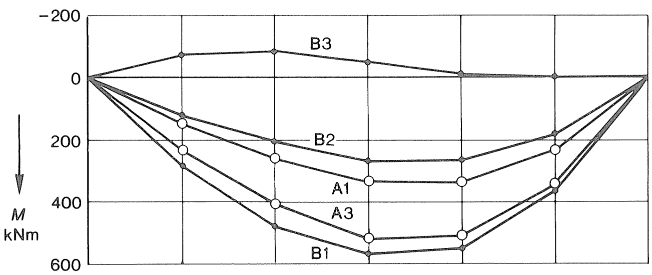

a.

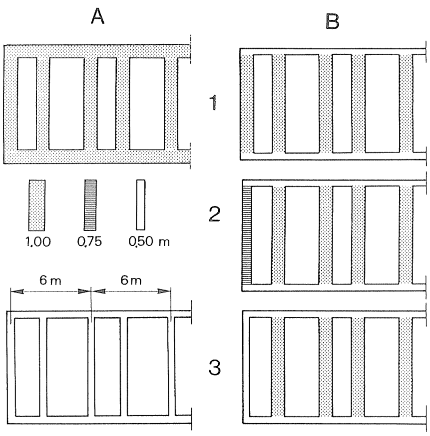

b.

Fig. 31.
Bending moments related to the width of the strip footings (homogeneous subsoil).
a. Bending moments for the cases shown in Fig. 30b. (The influence of the direct load transfer to the subsoil has been neglected).
b. Some footings width configurations.
   A. All footings the same width.
   B. Footing width under front and rear wall half that under transverse walls. Only the footing width of the end walls has been varied.

The bending moments according to Figs. 28 and 30 have been calculated for Case B1.

influence. In Case B the floor-bearing walls have footings which are twice the width of the footings of the longitudinal front and rear walls. The footing width of the end walls is variable, and this proves to have a large influence on the bending moments, see Cases B1-2-3, Fig. 31. The smaller the support given by the end walls, the smaller the bending moments in the terrace. One should notice that the magnitude of the bending moments varies strongly, but that the shape of these curves remains more or less the same.

4.6 *Maximum tensile stresses in the walls*

In this section the walls are treated as if they were composed of a homogeneous, isotropic and elastic material. The mechanical properties and the strength of masonry are dealt with in Section 4.7 and a proposal made for interpreting the results given in the present section.

As mentioned above in Section 4.5, the magnitude of bending moments in a terrace of houses is very dependent on the inhomogenities of the subsoil and the relative proportions of the width of the strip footings. As shown in Section 4.3, superimposing three basic loading cases gives detailed information about the stress distribution in the walls and in longitudinal walls with openings in particular.

Maximum stresses mostly occur at the edges of door and window openings and consequently the principal stresses work in horizontal and vertical directions. These stresses can, therefore be superimposed algebraically. An exception has to made, however, for the peak stresses in the immediate vicinity of the corners of these door and window openings, see Section 4.7.

In order to identify the areas where the maximum tensile stresses will occur, the stress distribution has been determined for a house in the centre of a terrace and another at the end. This has been done for some extreme, but still realistic moment combinations, see Fig. 32. In these figures only those tensile stresses have been shown which exceed a certain value. From these figures one or two points can be chosen, for each representative area, where the numerical value of the extreme tensile stresses can be plotted as a function of the bending moment.

In this way it is possible to find out the extent to which a terrace of houses is sensitive to cracking, depending of the particular circumstances. As mentioned above, the stiffness of the subsoil is small compared to the stiffness of the uncracked terrace. As a result, the extent to which there is a direct transfer of the load to the subsoil is rather insensitive to the stiffness of the subsoil and the corresponding stress distribution is hardly affected by change in soil stiffness. This means that all stresses in the walls, caused by Loading Case 3, Section 4.3, see Fig. 23a, remain constant even if the bending moment in the terrace increases. This is shown in Fig. 33a for a house at the end of a terrace. The stresses at some representative points of a front wall have been plotted in the figure. The transfer of the small remaining part of the load to the end walls by means of bending moments however, will cause stresses which are proportional to these bending moments, see Fig. 33b. These bending moments are basically the superposition of the Loading Cases 1 and 2 described in Section 4.3, as shown in Figs. 23b and 23c.

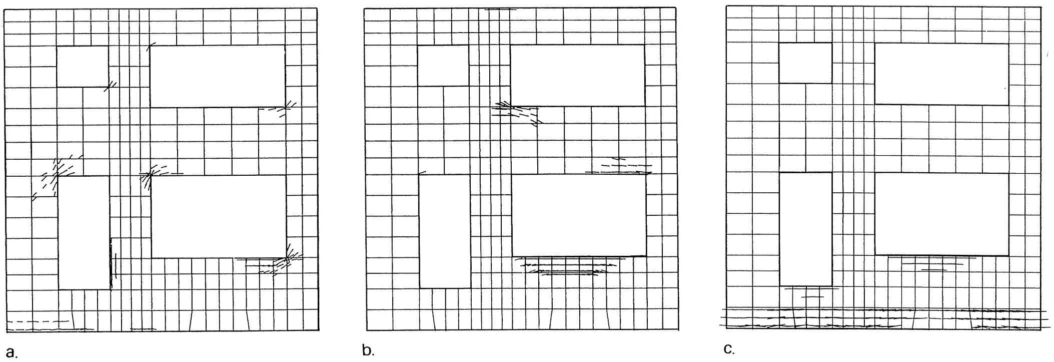

Fig. 32. Location of extreme tensile stresses for three loading cases.
a. The house at the left end of the terrace; direct load transfer to the subsoil $+ M_2 = 400$ kNm.
Only the principal tensile stresses which exceed $\sigma_1 = 0.25$ N/mm^2 are shown.
b. House at the centre of the terrace; direct load transfer to the subsoil only, $M_1 = 0$.
Only the principal tensile stresses which exceed $\sigma_1 = 0.125$ N/mm^2 are shown.
c. House at the centre of the terrace; direct load transfer $+ M_1 = 600$ kNm.
Only the principal tensile stresses which exceed $\sigma_1 = 0.25$ N/mm^2 are shown.

The final stress distribution in the wall is found by superimposing the results of Loading Cases 1, 2 and 3. For the representative points being considered this means superimposing the results of Figs. 33a and 33b. The result is shown in Fig. 33c; all stresses are linear functions of the bending moment, but they are no longer proportional to the bending moment.

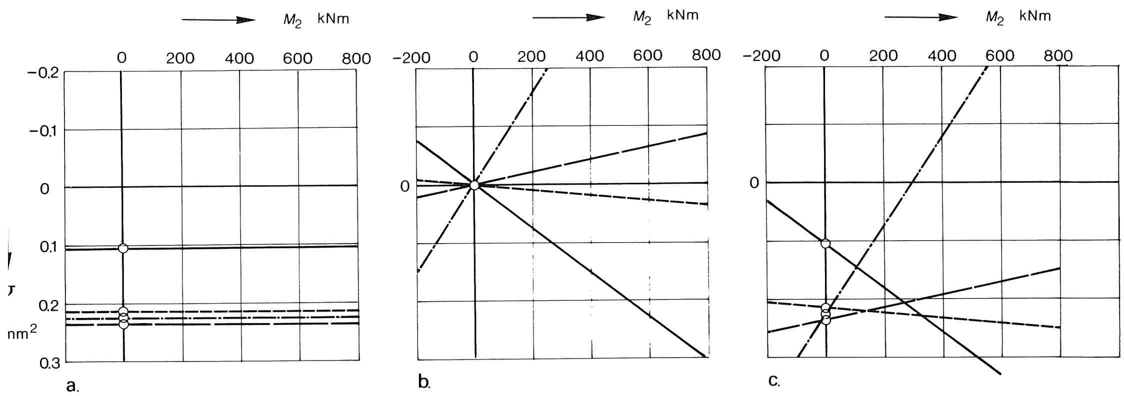

Fig. 33. Extreme tensile stresses at representative points of the walls of a house at the end of a terrace, as a function of the bending moment M_2.
a. Stresses due to Loading Case 3; direct transfer of the load to the subsoil.
b. Superposition of Loading Cases 1 and 2, linearly varying bending moment varying between 0 and M_2; (M_2 according to Fig. 22d).
c. Superposition of Fig. 33a and 33b; the tensile stresses are linear functions of, but not proportional to the bending moment.

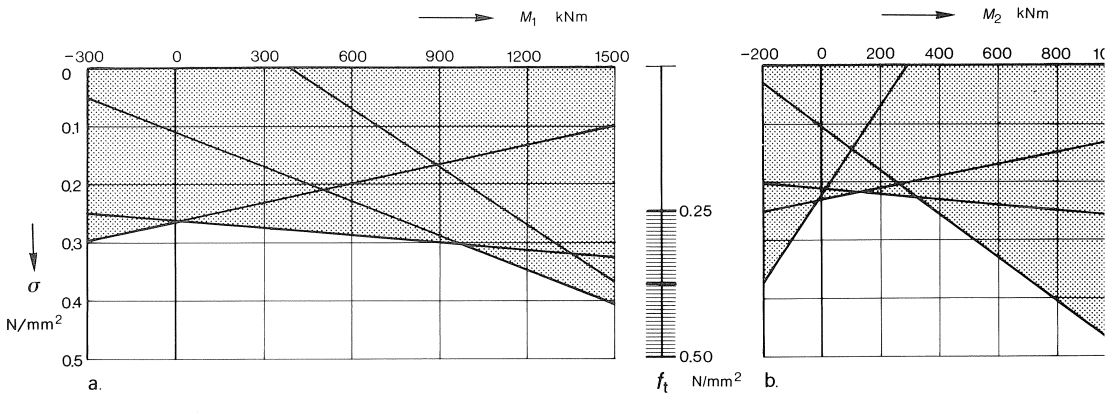

Fig. 34. Extreme tensile stresses in the walls of a terrace of houses as a function of the bending moment (M_1 and M_2, according to Fig. 22d).
a. House at the centre of the terrace.
b. House at the end of the terrace.
The variation in the tensile strength of the masonry used in these terrace houses is shown between Figs. a and b (95% and 5% probability of exceedance).

The results in Fig. 33c are also shown in Fig. 34b, the shaded area showing the magnitude of all the tensile stresses which can occur somewhere in the longitudinal walls of a house at the end of a terrace. The tensile stresses which can occur in a house in the middle of the terrace are shown in Fig. 34a.

If the magnitude of the bending moment increases or decreases, other areas of the walls become critical. It is striking that there is in fact a range of bending moments in which the extreme tensile stresses reach a minimum which is almost constant. This is due to the fact that the tensile stresses, which are caused by the bending moments, are compensated to a great extent by compressive stresses, which are caused by the direct load transfer to the subsoil. As soon as the positive bending moments exceed a certain value, however, or if they become negative, the tensile stresses increase more rapidly.

To obtain some idea when cracking is liable to occur, the variation in tensile strength of masonry has been plotted in between Figs. 34a and 34b. It is obvious that in the case of a house in the middle of the terrace, even in the most favourable circumstances ($-300 < M < +1000$ kNm) there is always a possibility of cracking. For a house at the end of the terrace, there is no possibility of cracking in the most favourable circumstances ($0 < M < 400$ kNm). However if the moment exceeds a value of $M = 1000$ kNm, then cracking will be almost inevitable.

4.7 *Properties of masonry*

Masonry is a stiff but brittle material, which is strong in compression but weak in tension. The compressive strength of masonry in the vertical or horizontal direction

varies between 8 and 16 N/mm^2, for the kind of masonry used in the part of the country being considered.
If masonry is loaded in tension, the behaviour depends of the direction of the tensile stresses relative to the direction of the joints. Vertical tensile stresses are shown in Fig. 35a. Cracking will occur as soon as the low bond strength is reached, this strength varying between 0.1 and 0.3 N/mm^2. Horizontal tensile stresses are shown in Fig. 35b. Since the bond strength at the vertical joints is easily exceeded, hair cracks develop very quickly but are overlooked most of the time. If the tensile stresses are increased further, the tensile forces have to be transmitted from one brick to another by shear stresses in the horizontal joints. The resulting deformations however, are much larger than those which occurred before the vertical hair cracks. This is shown schematically in Fig. 36. Continuous cracks can occur in two ways: through the joint and bricks, if the bricks are weak, or in a zig-zag shape along the joints if the bricks are strong, see Fig. 35c. The direction of the cracks under pure shear is shown in Fig. 35d, tensile stresses occurring at an angle of 45°. The resulting crack formation is then more or less perpendicular to these tensile stresses.
The compressive strength of masonry is never reached in terrace houses. Vertical tensile stresses are usually suppressed by vertical compressive stresses. The cracking patterns shown in Figs. 35c and 35d are typical of terrace houses.

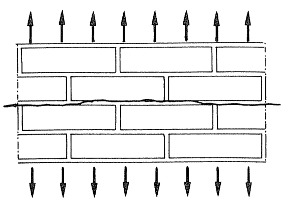
a.

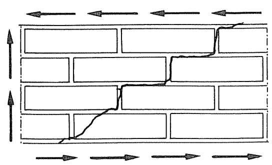
d.

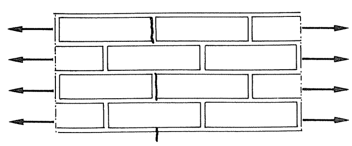
b.

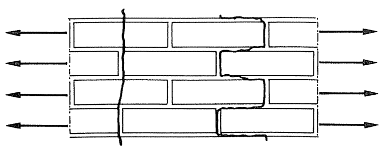
c.

Fig. 35.
Tensile strength of masonry.
a. Vertical tensile stresses cause cracks as soon as the bond strength in the joints is exceeded.
b. Horizontal tensile stresses initially cause discontinuous hair cracks in the vertical joints.
c. Continuous cracks can occur in two ways
   - through vertical joints and directly through bricks (left),
   - in a zig zag shape along vertical and horizontal joints (right).
d. Pure shear causes cracks which are more or less at 45°, mostly in a "staircase" shape.

In order to estimate the possibility of cracking, the variation in the tensile strength of masonry has to be known. An extensive study of the literature indicates the exceedance values for the tensile strength f_t, of typical masonry walls:

95% chance of exceedance $f_t = 0.250$ N/mm^2
50% chance of exceedance $f_t = 0.375$ N/mm^2 (mean value)
5% chance of exceedance $f_t = 0.500$ N/mm^2
standard deviation $s = 0.076$ N/mm^2

The Gaussian distribution of the tensile strength is shown in Fig. 37 and the schematized stress-strain relationship in Fig. 36.
It is assumed that crack formation will occur along the edges of the openings if the numerical value of the tensile stress is exceeded. For the peak stresses in the corners of the openings however, it is assumed that cracks will occur, if the tensile strain shown in Fig. 36 is exceeded and the corresponding imaginary elastic value for the stress has been introduced.

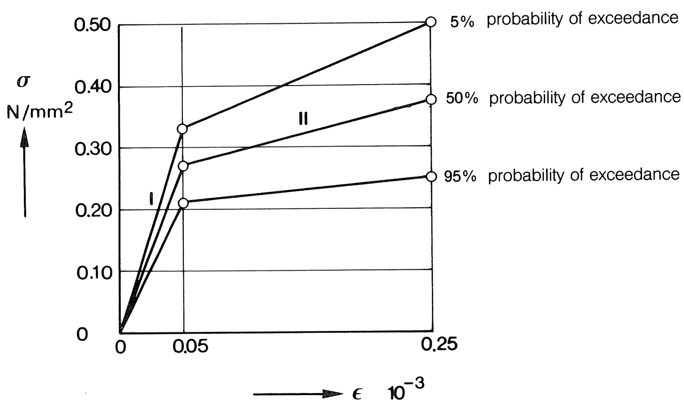

Fig. 36. Schematized stress-strain relationships for masonry under horizontal tension (95%, 50% and 5% probability of exceedance).
- Section I: before the development of hair cracks.
- Section II: after hair cracking and before continuous cracking.

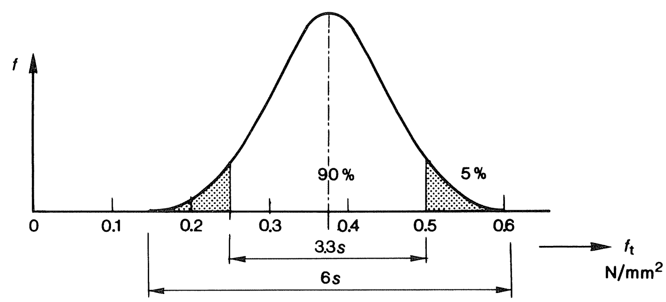

Fig. 37. Normal (Gaussian) distribution for the tensile strength of masonry.

5 Probabilistic approach to damage prediction

5.1 *Prediction of damage*

Damage in a built-up area cannot be predicted with certainty. However a prediction of the probability that damage will occur, can be given. In order to do this the variation in the properties of the parameters which govern the problem, has to be determined.
For a given case, the geometrical properties of the terrace of houses are known or easily determined. The geometry of the foundation however is usually not known precisely. This is also true for the properties of the subsoil and the tensile strength of the masonry. All these parameters are stochastic variables and an indication of the probability of cracking can be given by using a probabilistic approach.

5.2 *Determination of the stochastic variables*

The probability of cracking is determined, ultimately by only two stochastic variables: the extreme tensile stresses which will occur somewhere in the walls of the terrace, and the tensile strength of masonry. Tensile strength is treated in Section 4.7 but intermediate steps are required in order to determine the expected extreme tensile stresses.
Only one type of building has been considered in the investigation, the terrace of houses shown in Fig. 16a. This type of building has been considered as representative for the whole area. If there is a large variety of buildings in an area a number of representative buildings should be considered.
The geometry of the terrace has not been varied in the calculations. Various widths of the footing foundations have been considered however, because it has been found that the bending moments are rather sensitive to differences in these widths.
The properties of the subsoil are not known in detail and as a starting point for the calculations, it was assumed that the subsoil is completely homogeneous. This is the most favourable condition that can occur. As mentioned above in Section 4.1 the numerical value for the stiffness of the subsoil - between certain limits - is of minor importance to the stress distribution in the walls. Extreme values of subsoil stiffness can however be investigated.
Of much more importance are the horizontal variations in mechanical properties of the subsoil within the length of the terrace. Obviously relative variation of these properties should be known in detail. If one wants to be on the safe side and assumes a large variation in the mechanical properties of the subsoil, there is no doubt that cracking will occur in all buildings being considered.
The method for determining bending moments in a terrace has been explained in Section 4.2 and is illustrated in Figs. 28, 30 and 31. The extreme bending moments in the terrace can be found knowing the situation of the terrace of houses, the inhomogenities of the subsoil and the variation in foundation footings.
The next step is to assume that the extreme moments as determined above, relate to the situation with maximum and minimum probabilities of exceedance of 95% and 5%, which is typical in civil engineering, implying that the normal (Gaussian) distribution

is valid. The mean value and the standard deviation can therefore be determined from the extreme values of the bending moments

$$\left(\mu = \frac{M_1 + M_2}{2};\ s = \Delta M / 3.6\right).$$

The bending moments do not play an important role, in crack formation this role is reserved for the tensile stresses.
When the range in the bending moments is known, the variation in the extreme tensile stresses can be determined, from figures as for instance Fig. 34. The initial assumption which can be made is that the maximum and minimum value of the tensile stress in the range of moments being considered, are those with a 95% and 5% probability of exceedance, see Section 5.3. Another approach, however, which is preferable, is described in Section 5.4.

5.3 *Approach involving two stochastic variables*

No cracking will occur if the residual stress Z obeys the equation

$$Z = R - S > 0$$

in which:

R = normal distribution of the tensile strength of the masonry
S = normal distribution of the extreme tensile stress

If two stochastic variables have to be subtracted, the mean value of Z is equal to the difference of the mean values of R and S. If both quantities are independent of each other, the standard deviation of Z follows from $s_Z = \sqrt{s_R^2 + s_S^2}$.
The probability of cracking is determined in Fig. 38 for terraces of houses on inhomogeneous subsoil, using the procedure described in Section 5.2. The normal distribution of R (strength) and S (stress) overlap considerably and there is a large probability of cracking, due to the influence of dead weight alone. As mentioned in Section 5.2 the approach explained in Section 5.4 is peferable however.

5.4 *Approach involving one stochastic variable*

The degree of certainty about the magnitude of the bending moments increases with the amount of information available about the foundation and the properties of the subsoil. If the distribution of the bending moments in the terrace is known precisely, the extreme tensile stresses in the masonry can be treated as deterministic variables. Then the tensile strength of the masonry would remain as the only stochastic variable. If the bending moments are known, the corresponding extreme tensile stresses in all houses of the terrace are also known. As mentioned in Section 4.3, only the case of a house in the centre and at the end of the terrace have to be considered, since these are representative of all houses of the terrace.

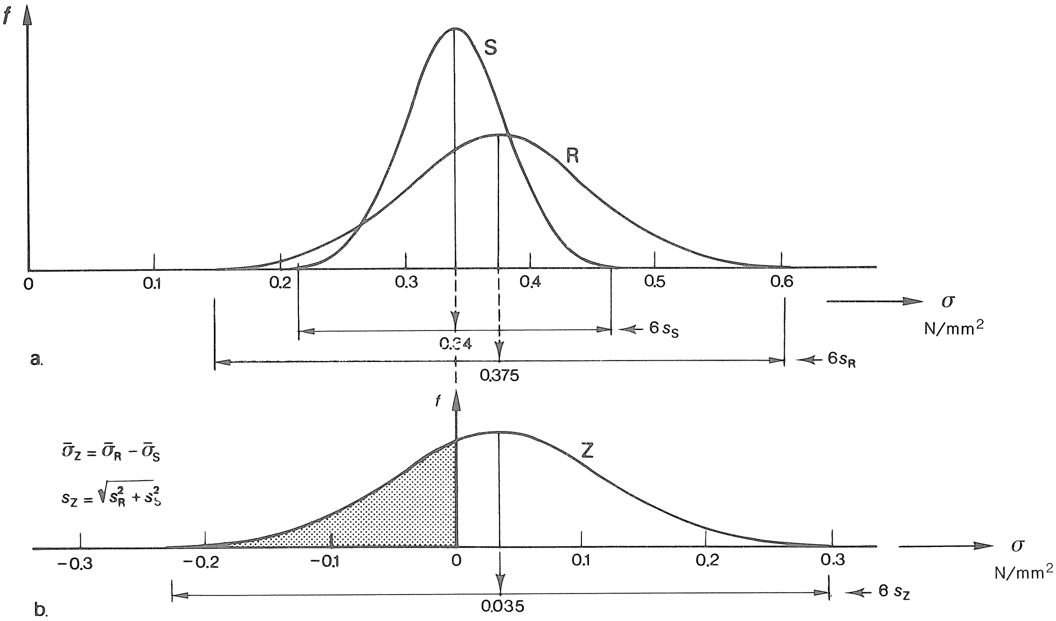

Fig. 38. Probability of cracking in a house at the centre of a terrace on inhomogeneous subsoil.
a. The normal distribution for *R* (strength) and *S* (stress) overlap considerably.
b. Determination of the residual strength *Z*. Probability of cracking equals 34%.

The shape of the bending moment curves for the terrace is such that the bending moment M_2 in a house at the end is, according to Fig. 22d, almost equal to $M_2 = \frac{2}{3}M_1$, where M_1 is the constant bending moment of a house in the centre of the terrace. This makes it possible to plot the extreme tensile stresses in both houses in one and the same figure, as a function of the bending moment M_1, see Fig. 39a. To check the validity of this assumption one should compare these moments for example in Fig. 31.
The next step is to calculate the probability of cracking using the approach given in Section 5.3, see Fig. 39b. The mean value is again equal to the difference of the mean values of the tensile strength and the extreme tensile stress, the standard deviation of the residual stress now being equal to the standard deviation of the tensile strength. The results of this probability calculation are shown schematically in Fig. 40. Most of the time the bending moments of a house in the centre of the terrace are representative of the terrace as a whole. The probability of cracking due to dead weight is about 10% for bending moments between 0 and + 900 kNm. As soon as the bending moments become negative, the probability of cracking increases. In addition if bending moments are larger than + 900 kNm this probability increases strongly. One should realize that these numerical bending moment values strongly depend on the assumptions about the stochastic qualities of the tensile strength, and even small changes in these assumptions can change the results considerably. The trend in the phenomena remains however

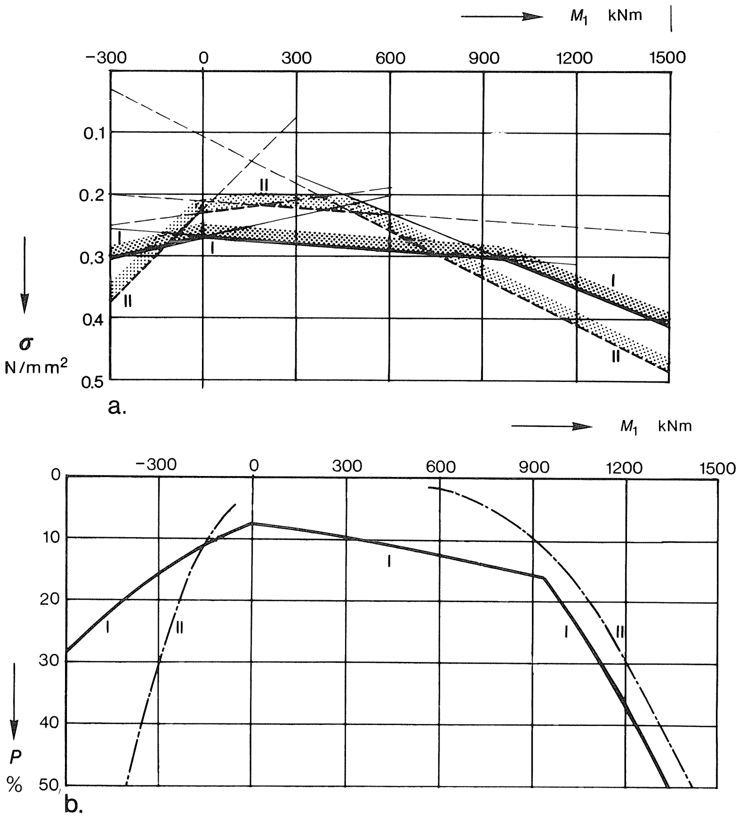

Fig. 39. Probability of cracking in the walls in a terrace of houses as a function of the maximum bending moment M_1.
a. Extreme tensile stresses in the front and rear walls of the terrace.
I House at the centre; II house at the end.
b. Probability of cracking P in %.

more or less the same, confirming the well known fact that long buildings are more vulnerable to damage by hogging than by sagging.

5.5 *Increased probability of cracking due to a fall in the groundwater level*

There is a certain moment distribution in the terrace caused by the transference of dead weight to the subsoil. This moment distribution will change if the groundwater level changes. From the calculations given in Sections 4.3 and 4.4 it follows that a lowering in ditch water level - below the lowest level ever reached - will produce an extra bending moment of − 100 kNm if the subsoil is homogeneous.
Due to the large variations in groundwater level which are caused by seasonable influence, these extra moments will vary between − 100 and + 100 kNm, see Fig. 28b. In the case of an inhomogeneous subsoil, a uniform fall in groundwater level of 0.20 m

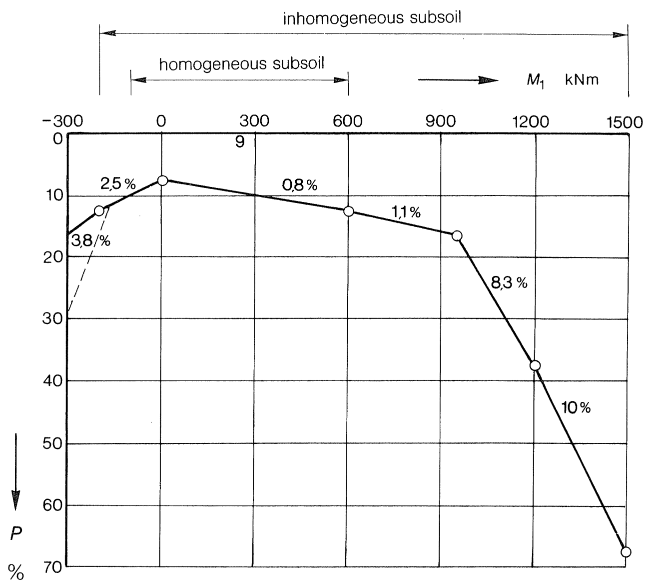

Fig. 40. The probability of cracking in a terrace of houses as a function of the maximum bending moment M_1, for bending moments caused by dead weight, shown schematically. The values on the various sections of the curve show the increase or decrease in the probability of cracking if the moment is increased or decreased by 100 kNm.

will cause extra bending moments which will vary between − 160 and + 100 kNm, for a house in the centre of the terrace, see Fig. 30b. From this figure it also follows that the bending moments in houses at the end of the terrace are very small and may be neglected.

If measures have to be taken to reduce the probability of damage, it is only necessary to consider the increase in probability, due to a fall in the groundwater level. The schematic curve in Fig. 40 is a good starting point for calculations. The procedure is explained below with the help of an example.

It is assumed that the bending moment in a house at the centre of the terrace is equal to $M = +300$ kNm, see Fig. 40, in which the probability of cracking due to dead weight alone is 10%. As a result of a fall in the groundwater level of 0.20 m, the bending moment will increase to

$M = +300 + 100 = +400$ kNm, but may also decrease to
$M = +300 - 160 = +140$ kNm.

If the bending moment is increased to 400 kNm, the probability of cracking increases to 10.8%, see Fig. 40. A decrease of the bending moment gives also a reduction in the probability of cracking and does not need to be considered.

Had the bending moment due to dead load however, been equal to + 1200 kNm, an increase of the bending moment to $M = +1300$ kNm, would have increased the probability of cracking from 37.5% to 47.5%, an increase of 10%.

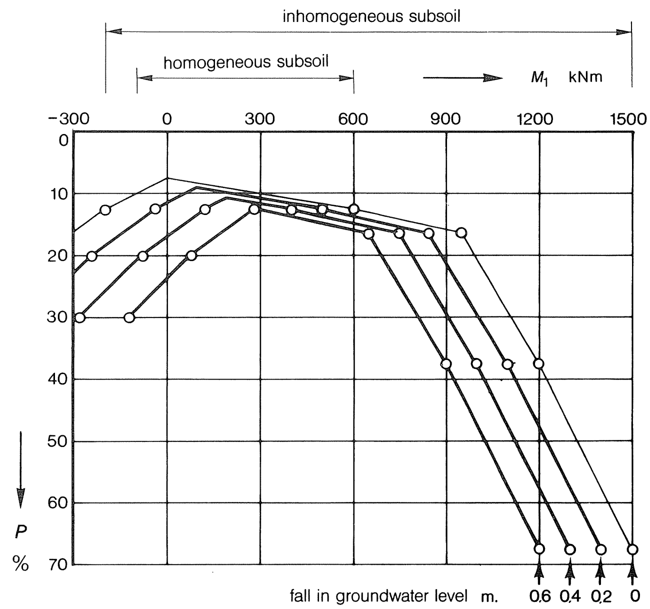

Fig. 41. The probability of cracking for the terrace of six houses, due to dead weight and a uniform fall in groundwater level of 0.20, 0.40 and 0.60 m. Calculations are for a subsoil consisting mainly of clay, with the terrace positioned in the most unfavourable position in relation to the inhomogeneities of the subsoil.

The calculations as given above can be avoided, if the curve for the probability of cracking is given a shift to the left over a distance equal to 100 kNm. This has been done in Fig. 41 and it is easily verified that the increased probability of cracking due to a lowering of the groundwater level can be read now under the bending moment belonging to dead weight alone.

For negative bending moments the curve for the probability of cracking has a slope in the opposite direction. In this case the bending moment of – 160 kNm should be considered and the corresponding branch of the curve has to be shifted to the right over a distance of 160 kNm.

In a similar way the increase of the probability of cracking can be determined for other falls in groundwater level. The effects for 0.40 m and 0.60 m are also shown in Fig. 41. With this approach it is not necessary to know the numerical value of the bending moment due to dead weight precisely because the slope of the curve, which remains constant over quite a range, is responsible for the increase in probability. In the gently sloping sections of the curve the increase in probability is less than 1% per 0.20 m fall in groundwater level. In unfavourable situations, however, where the bending moments due to dead weight are large, as in the case of an inhomogeneous subsoil, the increase in probability of cracking might increase to 10% per 0.20 m fall in groundwater level.

To obtain an indication if buildings are in the gently sloping part of the curve or not, one should find out if there have been previous falls in groundwater level and if any cracking occurred.

It should be realized also that a lowering of the water level in a ditch does not necessarily have a direct influence on cracking. The level of the groundwater can show considerable differences between summer and winter, without reaching the extreme levels shown in Fig. 2. Even if the ditch water level is lowered further, the extreme low groundwater level, for example, that which occurred in 1976, will not necessarily be reached. This might be the case for several years until there is another extremely dry summer.

The further the groundwater level falls, the smaller the gently sloping area of the probability curve will become. Attention should also be paid to the influence of trees with deep roots, which might lower the groundwater level further and will therefore contribute to cracking damage.

Finally it should be obvious that every fall in groundwater level, below the previously lowest level, will increase the probability of cracking. To obtain numerical values for a reasonable lower limit of groundwater level, groundwater levels have been assumed to be acceptable if the increase in probability of cracking in the most unfavourable situation, is less than 5%, more or less in agreement with normal building practice. It must be understood however, that this probability of exceedance is of a somewhat other nature.

6 References

1. Beranek, W. J. and G. Hannink, Mogelijkheid van schade aan de bebouwing door wijzigingen in het peil van polder- en boezemwater, Studieresultaten betreffende ongelijkmatige zakkingen in verband met aardgaswinning in de provincie Groningen, Commissie Bodemdaling door aardgaswinning, maart 1987.
2. Beranek, W. J. and G. Hobbelman, Interactie Grond–Gebouwen, Betonvereniging; S & E Publikatie 13, Funderingstechniek, 1985.
3. Beranek, W. J. and G. Hannink, Prediction of damage due to changes in groundwater level, 9th European Conference on Soil Mechanics and Foundation Engineering, Dublin, 1987.